with no peptide, followed by treatment for 24 h with 10 μM MG132 alone. These cells with ubiquitin-positive inclusions were co-stained with antibodies against pIκBα or IκBα.

Cell viability assay. Cell viability assay was performed using 2-(2-methoxy-4-nitrophenyl)-3-(4-nitrophenyl)-5-(2,4-disulfophenyl)-2H-tetrazolium monosodium salt assay, as described previously [25]. The differentiated SH-SY5Y cells were plated on a 96-well plate and incubated for 24 h at 37 °C in 5% CO_2. The cells were preincubated for 3 h with 40 μM of either wild-type or mutant NBD peptide, followed by treatment for 24 h with 40 μM of each NBD peptide in the presence or absence of 10 μM MG132. The cells were simultaneously preincubated for 3 h with no peptide, followed by treatment for 24 h with 10 μM MG132 alone. The live cell count was assayed using Cell Counting Kit-8 according to the instructions provided by Doujin (Cell Counting Kit-8; Kumamoto, Japan).

Statistical analysis. All data are expressed as means ± SEM. Comparisons between groups were performed using analysis of variance (Tukey's multiple *t* test).

A p value <0.05 indicated statistically significant differences.

Results

Phosphorylated IκBα and $SCF^{\beta\text{-}TrCP}$ complex are novel components of Lewy bodies

We first examined whether LB contain pIκBα and the components of $SCF^{\beta\text{-}TrCP}$ complex, which are major downstream components of the TNF-α signaling pathway. Immunohistochemical analysis revealed that anti-pIκBα and ROC1 antibodies predominantly recognized the LB in PD cases (Figs. 1A and B). Immunostaining with anti-NF-κB p65 antibody also showed the staining of LB (Fig. 1C). Anti-pIκBα and anti-ROC1 signals were strongly present in the halo region of LB, and the anti-NF-κB-p65 signal was present in the core region. In contrast, such immunoreactivities for pIκBα ROC1 and NF-κB were not observed in the control brains and when the primary antibody was omitted in PD and DLB brains (data not shown).

In the next step, the isolated LB were used to investigate whether these proteins are associated with LB. Confocal laser-scanning microscopic examination of sections prepared from freshly isolated LB from postmortem brains of DLB showed immunoreactivities for pIκBα, ROC1, Cul-1, and β-TrCP (Figs. 1D, G, J, and M). LB were identifiable by their strong α-synuclein staining in smears of isolated LB from DLB cortex (Figs. 1E, H, K, and N), but not in sections from a normal control cortex (data not shown). These immunoreactivities for the indicated antibodies in LB were distributed across or sometimes more concentrated in the central region of LB (Figs. 1F, I, L, and O). Counting of α-synuclein-positive LB indicated that 80–90% of the cortical LB ($n = 300$, pooled from three DLB cases) were also positive for ROC1 and Cul-1. A similar staining pattern was also observed in LB isolated from the substantia nigra (SN) of PD (data not shown).

Localization of pIκBα, ROC1, and Cul-1 in cytoplasmic inclusions of SH-SY5Y cells

As a model for the formation of cytoplasmic inclusions, we used SH-SY5Y cell lines treated with MG132 [26]. Localization of pIκBα, ROC1, and Cul-1 was investigated after the addition of 10 μM MG132 for 24 h in differentiated SH-SY5Y cells. Proteasomal dysfunction caused typical cytoplasmic inclusions that were stained with anti-ubiquitin (Ub) antibodies, and interestingly many, if not all, ubiquitinated inclusions were also positive for pIκBα, ROC1, and Cul-1 (Figs. 2A–C). Under normal conditions without MG132, the cells displayed low-level cytoplasmic staining for the indicated proteins (data not shown). Although we examined the effect of TNF-α on the formation of the inclusions, no inclusions that contained ubiquitin and pIκBα were observed after treatment with TNF-α alone. In addition, the effect of simultaneous treatment with TNF-α and MG132 was not significantly different from the results of MG132 treatment alone (data not shown).

We next examined whether these cells also contained α-synuclein in such cytoplasmic ubiquitinated inclusions. Following proteasomal inhibition with 10 μM MG132, some of the ubiquitinated cytoplasmic inclusions also exhibited α-synuclein immunoreactivity (Fig. 2D). Moreover, we examined whether pIκBα and components of the SCF complex colocalize with α-synuclein in the presence of 10 μM MG132. The α-synuclein-positive inclusions were also immunoreactive for pIκBα ROC1 and Cul-1 following treatment with 10 μM MG132 (Figs. 2E–G). The proportion of cells treated with 10 μM MG132 that contained aggregates immunoreactive for both pIκBα and α-synuclein was 7.98 ± 1.14%. In contrast, the proportion of 10 μM MG132-treated cells containing inclusions positive for both pIκBα and ubiquitin was 23.19 ± 3.84%, suggesting the relative low frequency of α-synuclein/pIκBα-containing inclusions (see Fig. 5B). Inclusions containing only ubiquitin, α-synuclein, or pIκBα were also noted, and their size was also comparatively heterogeneous (data not shown).

Inhibition of proteasomes increases phosphorylated IκBα level in SH-SY5Y cells

We examined the migration pattern of endogenous ubiquitin or pIκBα by SDS–PAGE in differentiated SH-SY5Y cells following proteasomal inhibition with MG132 and/or TNF-α for 24 h. Cells were treated as indicated in Fig. 3, and then the resulting cell extracts were separated into detergent-soluble and detergent-insoluble fractions. Treatment with 10 μM MG132 resulted in accumulation of high-molecular weight ubiquitin–protein conjugates particularly within the insoluble fractions but not in TNF-α alone and control

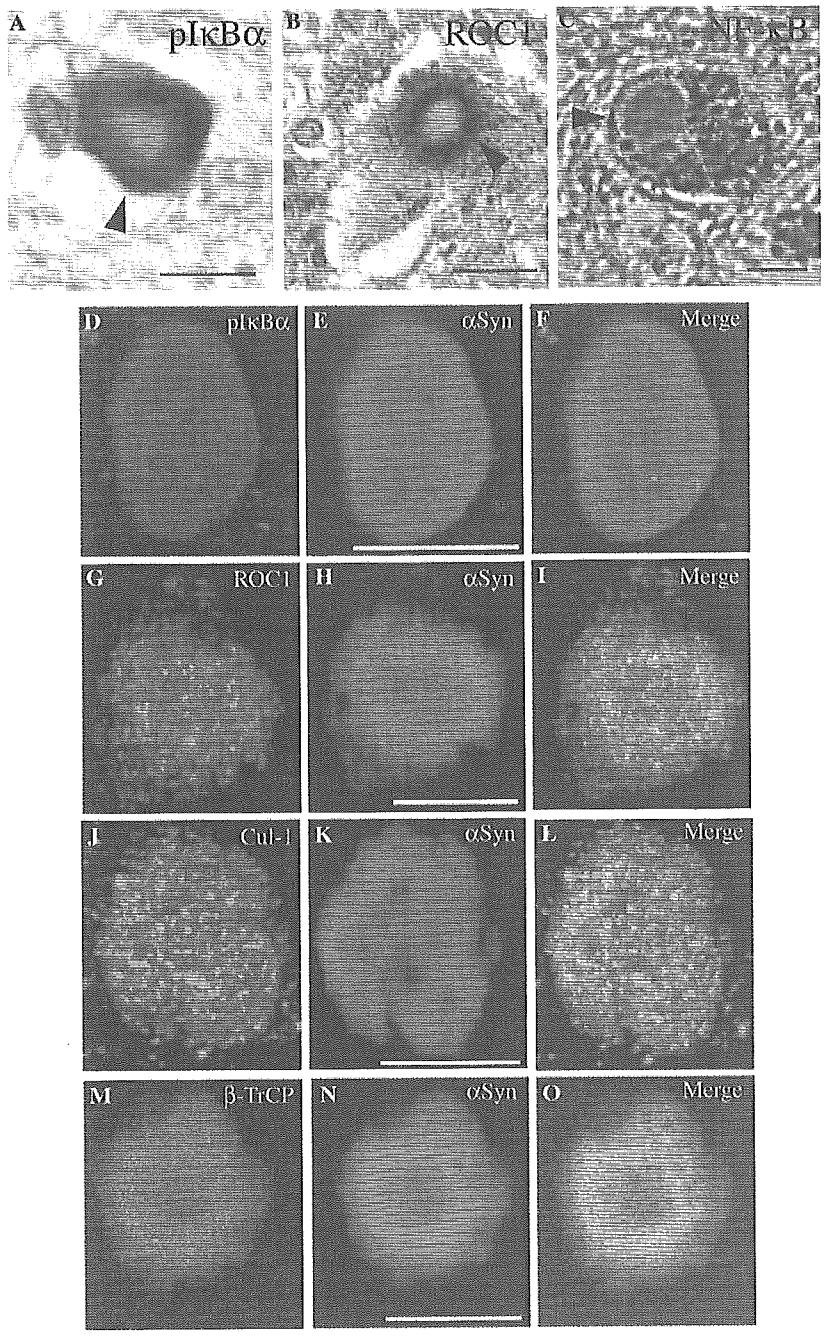

Fig. 1. Identification of phosphorylated IκBα and components of $SCF^{\beta\text{-}TrCP}$ in Lewy bodies. (Upper panel) Paraffin sections of autopsied human brain samples with PD were immunostained with antibodies against pIκBα (A), ROC1 (B), and NF-κB p65 (C). Lewy bodies are marked by arrowheads. Scale bars = 20 μm (A–C). (Lower panel) Colocalization of α-synuclein (αSyn), pIκBα, and components of $SCF^{\beta\text{-}TrCP}$ in isolated LB from DLB (Dementia with LB) cases. LB were identified by α-synuclein staining. Each preparation was doubly stained with sheep anti-α-synuclein (E, H, K, and N) and various antibodies against pIκBα (D), ROC1 (G), Cul-1 (J), and β-TrCP (M), and analyzed with a laser-scanning confocal microscope. Panels (F, I, L, and O) at right correspond to merged images; yellow-colored structures indicate colocalization. Scale bars = 10 μm (D–O).

cells (Fig. 3A). Unexpectedly, the effect of TNF-α was very weak in SH-SY5Y cells, because no massive reduction of IκBα was observed upon treatment with TNF-α for 1, 12, or 24 h (Fig. 3C and data not shown). This finding was in marked contrast to the almost complete disappearance of IκBα in HeLa cells treated with 20 ng/ml TNF-α within 1 h (data not shown). However, TNF-α significantly increased the pIκBα level (Fig. 3B), indicating the existence of TNF-α response to a lesser extent in SH-SY5Y cells. It is of note that MG132 alone

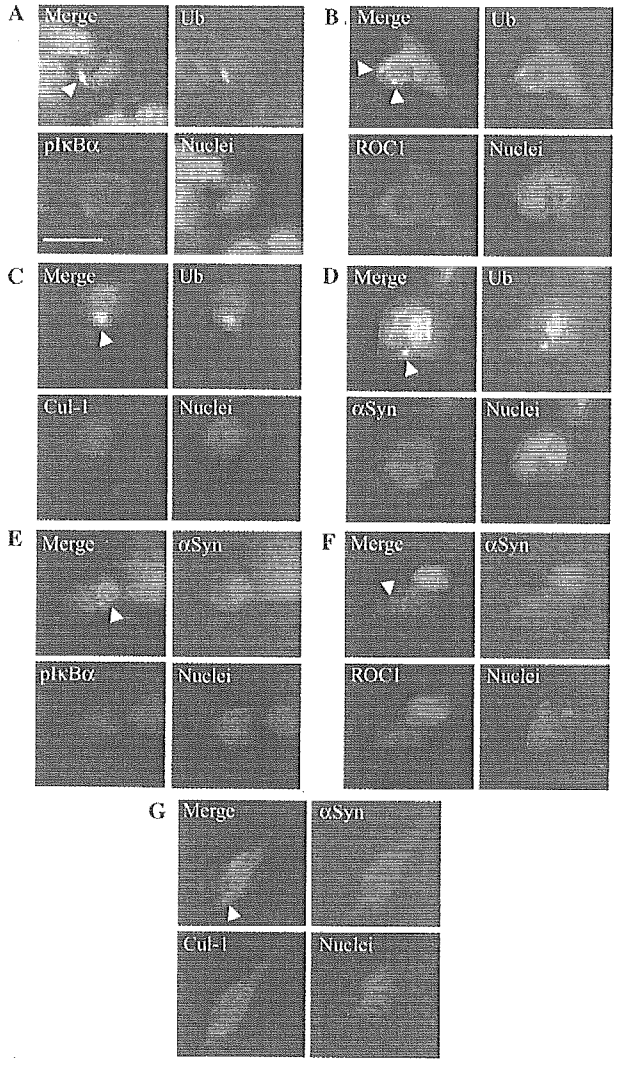

Fig. 2. Proteasomal inhibition leads to formation of pIκBα-positive cytoplasmic inclusions in SH-SY5Y cells. Differentiated SH-SY5Y cells were treated with 10 μM MG132 for 24 h, fixed and then double-stained with various combinations of antibodies as indicated. (A–D) Cytoplasmic inclusions positive for ubiquitin (Ub) were co-stained for pIκBα (A), ROC1 (B), Cul-1 (C), and α-synuclein (D). Arrowheads indicate the inclusions. Regions of overlap between ubiquitin (green) and immunoreactivities of the indicated proteins (red) appear in yellow color. (E–G) α-Synuclein (αSyn)-positive cytoplasmic inclusions were co-stained for pIκBα (E), ROC1 (F), and Cul-1 (G). Regions of overlap between α-synuclein (green) and immunoreactivities of the indicated proteins (red) appear in yellow color. Scale bar = 10 μm.

increased the pIκBα level in the cells (Fig. 3B), although additive effects of TNF-α and MG132 were not observed for phosphorylation of IκBα. Intriguingly, when detergent-soluble and -insoluble fractions were immunoblotted with anti-pIκBα or anti-IκBα antibody, both proteins were clearly detected in the detergent-insoluble fraction after treatment with 10 μM MG132 but not in TNF-α alone and control cells (Figs. 3B and C). In addition, simultaneous treatment with TNF-α and MG132 had no significant effects in comparison with MG132

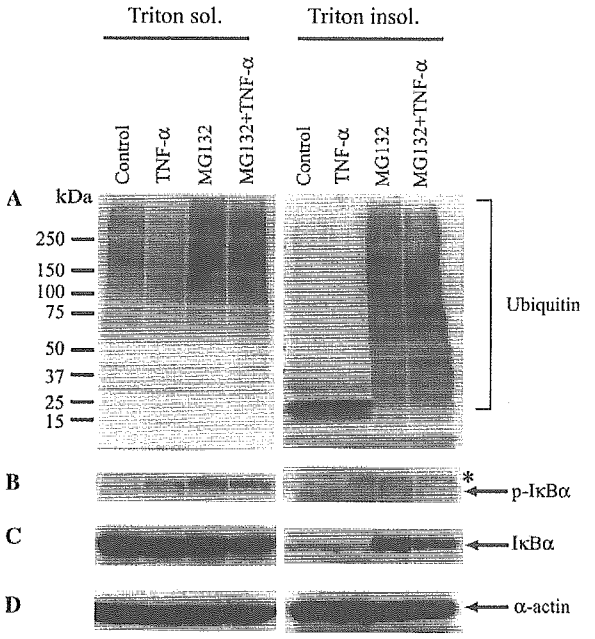

Fig. 3. Inhibition of the proteasome results in accumulation of pIκBα within the detergent-insoluble fraction of SH-SY5Y cells. The cells were treated for 24 h with 10 μM MG132 and/or 20 ng/ml TNF-α, and the cell lysates were processed for Western blotting, as described in Materials and methods. The protein was blotted onto PVDF membranes and probed with antibodies against ubiquitin (A), pIκBα (B), and IκBα (C). Note that anti-IκBα antibody reacted both phosphorylated and unphosphorylated forms. α-Actin served as a loading control (D). Asterisk indicates a non-specific band.

treatment alone. Thus, it is clear that IκBα, perhaps its phosphorylated form, is incorporated into the detergent-insoluble fraction under the conditions of proteasome inhibition.

The NBD peptide inhibits pIκBα entry into cytoplasmic ubiquitin-positive inclusions

The presence of pIκBα in LB of autopsied brains of PD patients and ubiquitinated inclusions in SH-SY5Y in the present study led us to examine whether inhibition of IKK, which phosphorylates IκBα, alters the processes of inclusion formation and cell death. First, we determined the optimal concentration of the cell-permeable NBD peptide, which is known to block the activity of IKK. To study the effect of NBD, SH-SY5Y cells were pre-treated with various concentrations of wild-type NBD for 3 h and then stimulated by 20 ng/ml TNF-α. In the present study, we used 40 μM NBD as the optimal concentration to block phosphorylation of IκBα. We also examined the effect of high concentrations of the NBD peptide (about 1000 μM), as described previously [21], but peptide toxicity was observed in our cell lines.

We next treated the cells with MG132 in the presence or absence of NBD peptide and then performed double

staining using antibodies for pIκBα, IκBα, and ubiquitin. Ubiquitinated inclusions containing pIκBα were identified in cells treated with MG132 alone or with MG132 in the presence of mutant NBD lacking inhibitory activity for IKK. On the other hand, while ubiquitinated inclusions were observed in cells treated with MG132 in the presence of wild-type NBD, only a few cells contained ubiquitinated inclusions positive for pIκBα (Fig. 4A). In addition, the use of an antibody

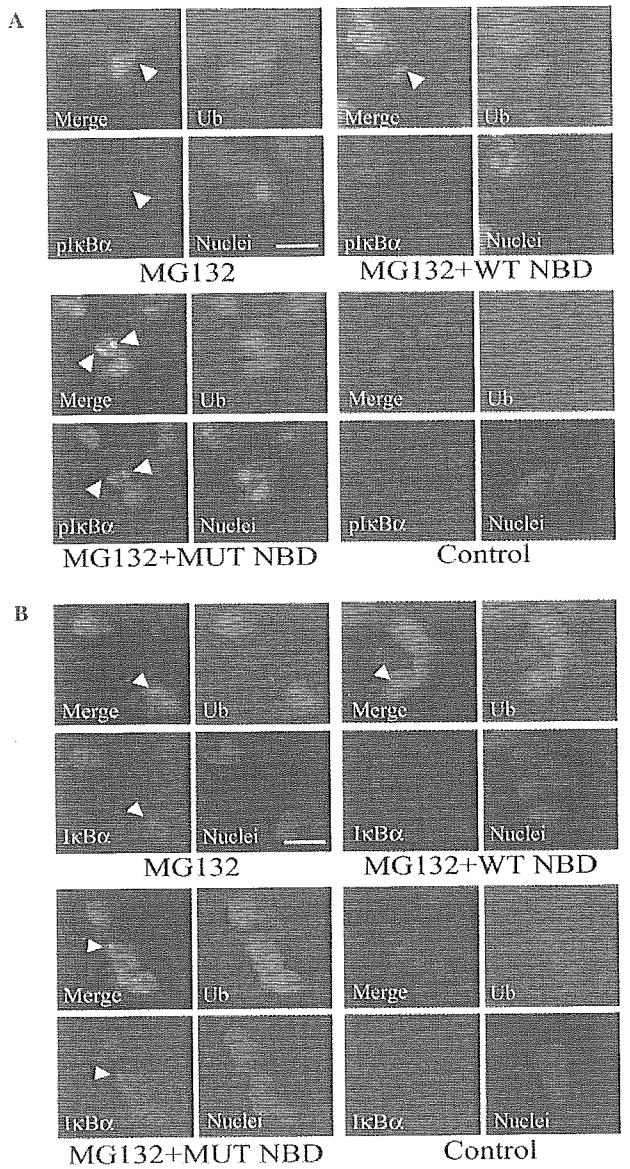

Fig. 4. Wild-type NBD decreases pIκBα level within the ubiquitinated inclusions in SH-SY5Y cells. The cells were treated for 24 h with 10 μM MG132 alone, or with 10 μM MG132 in the presence of 40 μM of either wild-type (WT NBD) or mutant NBD peptide (MUT NBD) as indicated in Materials and methods. Cells with ubiquitinated inclusions were co-stained with pIκBα (A) and IκBα (B). Arrowheads indicate the ubiquitinated inclusions. Regions of overlap between ubiquitin (green) and immunoreactivities of the indicated proteins (red) are shown in yellow color. Scale bar = 20 μm.

for IκBα in the presence of wild-type NBD was also associated with reduced number of cells with ubiquitinated inclusions positive for IκBα, compared with those treated with MG132 or MG132 in the presence of mutant NBD (Fig. 4B), indicating that phosphorylation of IκBα may be required for its incorporation into cytoplasmic inclusions generated by proteasome inhibition.

We then counted the number of cells with aggregated immunoreactivity for both ubiquitin and pIκBα antibodies under basal condition and following treatment with 10 μM MG132 with or without NBD peptide. It is worth noting that whereas approximately 50% of total cells contained ubiquitin-positive inclusions, pIκBα-positive inclusions were below 25% (Figs. 5A and B), suggesting that pIκBα is not incorporated into all inclusions. Wild-type NBD significantly decreased the number of cells with ubiquitinated inclusions (Fig. 5A, $p < 0.05$), and cells with cytoplasmic inclusions positive for pIκBα and ubiquitin, compared with cells treated with MG132 alone (Fig. 5B, $p < 0.001$). In comparison, mutant NBD did not show the same effects on phosphorylation of IκBα as wild-type NBD. Finally, we examined the toxicity of 10 μM MG132 on these cell lines. Treatment with 10 μM MG132 reduced cell viability to 37.84 ± 1.46%. In contrast, wild-type NBD did not influence cell viability under proteasomal inhibition (Fig. 5C).

Discussion

The appearance of LB in SN is a prominent feature in PD, but the pathogenic role of such inclusions remains elusive. In this study, we identified novel components including pIκBα and components of $SCF^{\beta\text{-}TrCP}$ ligase in LB. To date, several studies have reported that the UPP-related proteins (such as ubiquitin, the 20S proteasome subunit, and HSP70) are localized in LB of PD [27,28]. These findings indicate that there appears to be an important correlation between some pathological alteration in UPP and the formation of LB in PD. In this regard, the pathogenic nature of proteasomal dysfunction has been studied in experimental models using a proteasome inhibitor. It has been demonstrated that inhibition of proteasomal function induces the formation of cytoplasmic inclusions immunoreactive for ubiquitin and α-synuclein in PC12 cells and mesencephalic cultures [20,29]. These observations suggest that proteasomal dysfunction is associated with the development of cytoplasmic inclusions that may have features similar to those of LB, in terms of containing two proteins; i.e., α-synuclein and ubiquitin, described as the major components of LB [2].

pIκBα and SCF ligase are also involved in UPP-related proteins, and these molecules have not been adequately studied in PD. Therefore, to explore how these

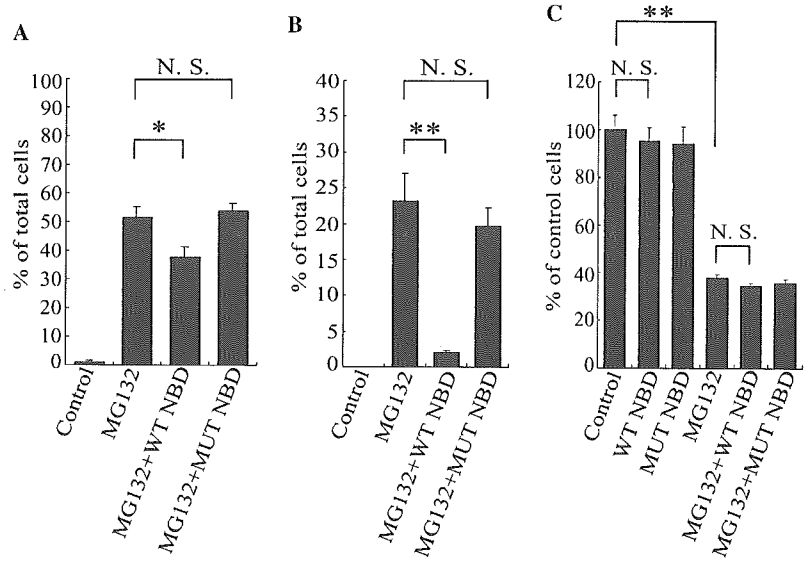

Fig. 5. Effects of NBD on formation of pIκBα-containing inclusions and cell death caused by proteasomal inhibition. After the cells were treated as explained in Fig. 4, the proportions of cells with cytoplasmic inclusions were determined. (A) The proportion of cells with ubiquitin-positive inclusions was calculated relative to total cells. (B) The proportion of cells with ubiquitinated inclusions containing pIκBα was calculated relative to total cells. In each experiment, 10 fields of 50 cells were counted. Similar effects of NBD were seen in two or more independent experiments. Data are means ± SEM. $*p < 0.05$; $**p < 0.001$ for differences between cell lines (Tukey's multiple t test). NS, not significant. (C) Cell viability was assessed as described in Materials and methods, and is expressed as the percentage of untreated cells. Similar results were seen in three independent experiments. Values are means ± SEM, each $n = 8$. $**p < 0.001$ for differences between cell lines (Tukey's multiple t test).

molecules are present in LB would be important in considering the process of LB formation. In our cell culture model, inhibition of normal proteasomal function by MG132 also induced the formation of ubiquitinated cytoplasmic inclusions containing α-synuclein, and this finding is consistent with previous reports [20,29], as described above. Intriguingly, our results showed that these inclusions were positive for pIκBα and some components of its ligase that are found in the LB. These findings suggest that the existence of pIκBα in LB is more likely and proteasomal dysfunction is an important factor in the formation of cytoplasmic inclusions.

Using SDS–PAGE analysis of detergent-soluble and -insoluble fractions, we found high-molecular weight ubiquitinated proteins particularly in the detergent-insoluble fraction, and pIκBα in the insoluble fraction following proteasomal inhibition with MG132. In contrast, after incubation with TNF-α alone, neither high-molecular weight ubiquitinated bands nor pIκBα was detected in the insoluble fractions, and cytoplasmic inclusions containing ubiquitin and pIκBα were not observed. These findings suggest that phosphorylation of IκBα alone is insufficient for the formation of cytoplasmic inclusions, and there appears to be a strong causal link between the accumulation of poorly degraded proteins, resulting from proteasomal dysfunction, and the formation of cytoplasmic inclusions.

We also showed that the presence of pIκBα in the ubiquitinated inclusions was markedly inhibited by a specific IKK inhibitor, under the conditions of MG132 treatment. This finding also supports the above-mentioned data that pIκBα is involved in the cytoplasmic inclusions resulting from proteasomal inhibition in our SH-SY5Y cells. In addition, this finding provides us a further possibility. In some neurodegenerative disorders, the ubiquitin-positive inclusions are considered to involve the ubiquitin–protein conjugates [28,30]. However, it is not clear which types of proteins are directly polyubiquitinated in LB. IκBα is phosphorylated by IKK, and pIκBα is polyubiquitinated by the $SCF^{\beta\text{-}TrCP}$, then degraded by the 26S proteasome. Thus, it is conceivable that once phosphorylation of IκBα is inhibited, neither polyubiquitination after its phosphorylation nor accumulation of IκBα into inclusion bodies is observed. We demonstrated that wild-type NBD peptide reduced the proportion of not only ubiquitin-positive inclusions, but also ubiquitinated inclusions containing pIκBα. Based on our finding, it is possible that the polyubiquitination of pIκBα resulting from proteasomal dysfunction triggers its entry into ubiquitinated cytoplasmic inclusions.

It is still not clear whether LB are cytoprotective or cytotoxic for neurons in the SN of PD. Recent studies suggest that the formation of protein aggregates or intracellular inclusions may be beneficial for cell survival rather than enhance cell death [31,32]. In the present study, exposure to MG132 alone or MG132 in the presence of wild-type NBD peptide did not alter cell viability whereas the same conditions decreased the ubiquitinated cytoplasmic inclusions. This finding at least supports the

conclusion of the above studies [31,32], i.e., the formation of cytoplasmic inclusions is not a toxic response against cell survival. Viewed from a different angle, our finding may suggest that inclusion bodies formed following proteasomal inhibition are independent of cell death.

In conclusion, we demonstrated the presence of pIκBα in LB of PD, and that similar inclusion bodies are produced in the presence of significant proteasomal dysfunction in cultured cells. Our observations in cultured cells may reflect, at least in part, the formation of LB in dopaminergic neurons of PD.

Acknowledgments

The authors thank Drs. Hideo Fujiwara and Takeshi Iwatsubo (University of Tokyo) for providing excellent advice. This study was supported by grants from the Ministry of Education, Science, Sports and Culture of Japan, by the Fund for "Research for the Future" Program from the Japan Society for the Promotion of Science. This study was also supported by funds from the NH&MRC and Michael J Fox Foundation.

References

[1] T. Iwatsubo, H. Yamaguchi, M. Fujimuro, H. Yokosawa, Y. Ihara, J.Q. Trojanowski, V.M. Lee, Purification and characterization of Lewy bodies from the brains of patients with diffuse Lewy body disease, Am. J. Pathol. 148 (1996) 1517–1529.

[2] M.G. Spillantini, M.L. Schmidt, V.M. Lee, J.Q. Trojanowski, R. Jakes, M. Goedert, α-Synuclein in Lewy bodies, Nature 388 (1997) 839–840.

[3] S.J.S. Berke, H.L. Paulson, Protein aggregation and the ubiquitin proteasome pathway: gaining the UPPer hand on neurodegeneration, Curr. Opin. Genet. Dev. 13 (2003) 253–261.

[4] K.S. McNaught, R. Belizaire, O. Isacson, P. Jenner, C.W. Olanow, Altered proteasomal function in sporadic Parkinson's disease, Exp. Neurol. 179 (2003) 38–46.

[5] G.K. Tofaris, A. Razzaq, B. Ghetti, K.S. Lilley, M.G. Spillantini, Ubiquitination of α-synuclein in Lewy bodies is a pathological event not associated with impairment of proteasome function, J. Biol. Chem. 278 (2003) 44405–44411.

[6] G. Boka, P. Anglade, D. Wallach, F. Javoy-Agid, Y. Agid, E.C. Hirsch, Immunocytochemical analysis of tumor necrosis factor and its receptors in Parkinson's disease, Neurosci. Lett. 172 (1994) 151–154.

[7] T. Nagatsu, M. Mogi, H. Ichinose, A. Togari, Changes in cytokines and neurotrophins in Parkinson's disease, J. Neural Transm. Suppl. 60 (2000) 277–290.

[8] H. Suzuki, T. Chiba, T. Suzuki, T. Fujita, T. Ikenoue, M. Omata, K. Furuichi, H. Shikama, K. Tanaka, Homodimer of two F-box proteins βTrCP1 or βTrCP2 binds to IκBα for signal-dependent ubiquitination, J. Biol. Chem. 275 (2000) 2877–2884.

[9] M. Karin, Y. Ben-Neriah, Phosphorylation meets ubiquitination: the control of NF-κB activity, Annu. Rev. Immunol. 18 (2000) 621–663.

[10] P. Strack, M. Caligiuri, M. Pelletier, M. Boisclair, A. Theodoras, P. Beer-Romero, S. Glass, T. Parsons, R.A. Copeland, K.R. Auger, P. Benfield, L. Brizuela, M. Rolfe, SCF(β-TRCP) and phosphorylation dependent ubiquitination of IκBα catalyzed by Ubc3 and Ubc4, Oncogene 19 (2000) 3529–3536.

[11] A.S. Baldwin Jr., The NF-κB and IκB proteins: new discoveries and insights, Annu. Rev. Immunol. 14 (1996) 649–683.

[12] T. Togo, E. Iseki, W. Marui, H. Akiyama, K. Ueda, K. Kosaka, Glial involvement in the degeneration process of Lewy body-bearing neurons and the degradation process of Lewy bodies in brains of dementia with Lewy bodies, J. Neurol. Sci. 184 (2001) 71–75.

[13] J.L. Biedler, S. Roffler-Tarlov, M. Schachner, L.S. Freedman, Multiple neurotransmitter synthesis by human neuroblastoma cell lines and clones, Cancer Res. 38 (1978) 3751–3757.

[14] S.I. Kubo, T. Kitami, S. Noda, H. Shimura, Y. Uchiyama, S. Asakawa, S. Minoshima, N. Shimizu, Y. Mizuno, N. Hattori, Parkin is associated with cellular vesicles, J. Neurochem. 78 (2001) 42–54.

[15] M. Sharma, P. Sharma, H.C. Pant, CDK-5-mediated neurofilament phosphorylation in SHSY5Y human neuroblastoma cells, J. Neurochem. 73 (1999) 79–86.

[16] H. Braak, D. Sandmann-Keil, W. Gai, E. Braak, Extensive axonal Lewy neurites in Parkinson's disease: a novel pathological feature revealed by α-synuclein immunocytochemistry, Neurosci. Lett. 265 (1999) 67–69.

[17] T. Kawakami, T. Chiba, T. Suzuki, K. Iwai, K. Yamanaka, N. Minato, H. Suzuki, N. Shimbara, Y. Hidaka, F. Osaka, M. Omata, K. Tanaka, NEDD8 recruits E2-ubiquitin to SCF E3 ligase, EMBO J. 20 (2001) 4003–4012.

[18] J. Fukae, M. Takanashi, S. Kubo, K. Nishioka, Y. Nakabeppu, H. Mori, Y. Mizuno, N. Hattori, Expression of 8-oxoguanine DNA (OGG1) in Parkinson's disease and related neurodegenerative disorders, Acta Neuropathol., in press.

[19] P.H. Jensen, K. Islam, J. Kenny, M.S. Nielsen, J. Power, W.P. Gai, Microtubule-associated protein 1B is a component of cortical Lewy bodies and binds α-synuclein filaments, J. Biol. Chem. 275 (2000) 21500–21507.

[20] H.J. Rideout, K.E. Larsen, D. Sulzer, L. Stefanis, Proteasomal inhibition leads to formation of ubiquitin/α-synuclein-immunoreactive inclusions in PC12 cells, J. Neurochem. 78 (2001) 899–908.

[21] M.J. May, F. D'Acquisto, L.A. Madge, J. Glockner, J.S. Pober, S. Ghosh, Selective inhibition of NF-κB activation by a peptide that blocks the interaction of NEMO with the IκB kinase complex, Science 289 (2000) 1550–1554.

[22] D. Derossi, A.H. Joliot, G. Chassaing, A. Prochiantz, The third helix of the Antennapedia homeodomain translocates through biological membranes, J. Biol. Chem. 269 (1994) 10444–10450.

[23] H. Hall, E.J. Williams, S.E. Moore, F.S. Walsh, A. Prochiantz, P. Doherty, Inhibition of FGF-stimulated phosphatidylinositol hydrolysis and neurite outgrowth by a cell-membrane permeable phosphopeptide, Curr. Biol. 6 (1996) 580–587.

[24] M.J. May, R.B. Marienfeld, S. Ghosh, Characterization of the IκB-kinase NEMO binding domain, J. Biol. Chem. 277 (2002) 45992–46000.

[25] T. Ohuchida, K. Okamoto, K. Akahane, A. Higure, H. Todoroki, Y. Abe, M. Kikuchi, S. Ikematsu, T. Muramatsu, H. Itoh, Midkine protects hepatocellular carcinoma cells against TRAIL-mediated apoptosis through down-regulation of caspase-3 activity, Cancer 100 (2004) 2430–2436.

[26] Y. Imai, M. Soda, T. Murakami, M. Shoji, K. Abe, R. Takahashi, A product of the human gene adjacent to parkin is a component of Lewy bodies and suppresses Pael receptor-induced cell death, J. Biol. Chem. 278 (2003) 51901–51910.

[27] E. Lindersson, R. Beedholm, P. Hojrup, T. Moos, W. Gai, K.B. Hendil, P.H. Jensen, Proteasomal inhibition by α-synuclein filaments and oligomers, J. Biol. Chem. 279 (2004) 12924–12934.

[28] K.S. McNaught, P. Shashidharan, D.P. Perl, P. Jenner, C.W. Olanow, Aggresome-related biogenesis of Lewy bodies, Eur. J. Neurosci. 16 (2002) 2136–2148.
[29] K.S. McNaught, C. Mytilineou, R. Jnobaptiste, J. Yabut, P. Shashidharan, P. Jennert, W.C. Olanow, Impairment of the ubiquitin–proteasome system causes dopaminergic cell death and inclusion body formation in ventral mesencephalic cultures, J. Neurochem. 81 (2002) 301–306.
[30] H. Mori, J. Kondo, Y. Ihara, Ubiquitin is a component of paired helical filaments in Alzheimer's disease, Science 235 (1987) 1641–1644.
[31] C. O'Farrell, D.D. Murphy, L. Petrucelli, A.B. Singleton, J. Hussey, M. Farrer, J. Hardy, D.W. Dickson, M.R. Cookson, Transfected synphilin-1 forms cytoplasmic inclusions in HEK293 cells, Brain Res. Mol. Brain Res. 97 (2001) 94–102.
[32] F.P. Marx, C. Holzmann, K.M. Strauss, L. Lei, O. Eberhardt, E. Gerhardt, M.R. Cookson, D. Hernandez, M.J. Farrer, J. Kachergus, S. Engelender, C.A. Ross, K. Berger, L. Schols, J.B. Schulz, O. Riess, R. Kruger, Identification and functional characterization of a novel R621C mutation in the synphilin-1 gene in Parkinson's disease, Hum. Mol. Genet. 12 (2003) 1223–1231.

Available online at www.sciencedirect.com
SCIENCE DIRECT®
Biochemical and Biophysical Research Communications 332 (2005) 233–240
BBRC
www.elsevier.com/locate/ybbrc

Common anti-apoptotic roles of parkin and α-synuclein in human dopaminergic cells

Yutaka Machida [a,b], Tomoki Chiba [b], Atsushi Takayanagi [f], Yoshikazu Tanaka [b,c], Masato Asanuma [d], Norio Ogawa [d], Akihiko Koyama [e], Takeshi Iwatsubo [e], Shosuke Ito [h], Poul Hening Jansen [g], Nobuyoshi Shimizu [f], Keiji Tanaka [b], Yoshikuni Mizuno [a], Nobutaka Hattori [a,*]

[a] *Department of Neurology, Juntendo University School of Medicine, Tokyo, Japan*
[b] *Department of Molecular Oncology, The Tokyo Metropolitan Institute of Medical Science, Tokyo, Japan*
[c] *Department of Veterinary Hygiene, Nippon Veterinary and Animal Science University, Tokyo, Japan*
[d] *Department of Brain Science, Okayama University Graduate School of Medicine and Dentistry, Okayama, Japan*
[e] *Department of Neuropathology and Neuroscience, Graduate School of Pharmaceutical Sciences, University of Tokyo, Japan*
[f] *Department of Molecular Biology Keio University, Tokyo, Japan*
[g] *Department of Neurology, Zlekenhuls Gelderse Vallei, Edo, Netherlands*
[h] *Fujita Health University School of Health Sciences, Aichi, Japan*

Received 17 April 2005
Available online 30 April 2005

Abstract

Parkin, a product of the gene responsible for autosomal recessive juvenile parkinsonism (AR-JP), is an important player in the pathogenic process of Parkinson's disease (PD). Despite numerous studies including search for the substrate of parkin as an E3 ubiquitin–protein ligase, the mechanism by which loss-of-function of parkin induces selective dopaminergic neuronal death remains unclear. Related to this issue, here we show that antisense knockdown of parkin causes apoptotic cell death of human dopaminergic SH-SY5Y cells associated with caspase activation and accompanied by accumulation of oxidative dopamine (DA) metabolites due to auto-oxidation of DOPA and DA. Forced expression of α-synuclein (α-SN), another familial PD gene product, prevented accumulation of oxidative DOPA/DA metabolites and cell death caused by parkin loss. Our findings indicate that both parkin and α-SN share a common pathway in DA metabolism whose abnormality leads to accumulation of oxidative DA metabolites and subsequent cell death.

Keywords: Parkin; Apoptosis; Antisense; Knockdown; Neuroblastoma; Synuclein dopamine metabolism; Quinone

Parkinson's disease (PD) is the second most common neurodegenerative disorder primarily caused by selective loss of dopaminergic neurons in the midbrain substantia nigra pars compacta. Familial PD has been highlighted to study the mechanisms underlying neurodegeneration in PD, although only 5–10% of patients with PD are of the familial form of PD [1,2]. To date, 10 causative genes have been mapped and cloned in familial PD by linkage studies, which have significantly enhanced our understanding of the genetic mechanisms of PD [3]. Of these genes, *parkin*, the causative gene (*PARK2*) of AR-JP, representing the most prevalent form of familial PD [4], is of special interest, because it encodes an E3 ubiquitin–protein ligase [5], which

* Corresponding author. Fax: +81 3 5800 0547.
E-mail address: nhattori@med.juntendo.ac.jp (N. Hattori).

0006-291X/$ - see front matter © 2005 Elsevier Inc. All rights reserved.
doi:10.1016/j.bbrc.2005.04.124

covalently attaches ubiquitin to target proteins, designating them for destruction by the proteasome [6,7]. These findings suggest that impediment of *parkin* leads to deterioration of dopaminergic neurons and that PD, at least AR-JP, is caused by the failure of proteolysis mediated by the ubiquitin–proteasome system [8]. Since then, our knowledge about parkin has expanded, and indeed at present various putative substrates, e.g., CDCrel-1, synphilin-1, α-SN22 (O-glycosylated form of α-synuclein [α-SN]), Pael-R, and cyclin E have been identified [9–14]. Moreover, negative regulation of parkin E3 activity by parkin modification, such as nitration and phosphorylation, has been reported [15–17], but the pathophysiological role of parkin is still poorly understood.

One crucial issue that needs to be investigated is why AR-JP brains show severe neuronal loss with gliosis in the substantia nigra and mild neuronal loss in the locus coeruleus and why dopaminergic neurons in the substantia nigra are particularly vulnerable to the loss-of-function effect of parkin, though parkin is expressed ubiquitously throughout the brain. To define how the loss-of-function of parkin induces selective dopaminergic neuronal death in the midbrain, we interfered with endogenous parkin mRNA, a potentially suitable in vitro model of AR-JP for investigating the mechanism of selective dopaminergic neuronal death. To knock down the level of parkin in cells, we designed a full-length human parkin antisense (abbreviated as-parkin) using an adenovirus vector that has a high multiplicity of infection (moi) toward post-mitotic cells or cell lines which has neuronal characteristics and is an excellent tool to search for the effect of as-parkin on differentiated SH-SY5Y cells that exhibit features characteristic of dopaminergic neurons.

Here, we report that as-parkin selectively induced apoptosis of SH-SY5Y cells in a caspase-dependent manner. We also found that loss of parkin resulted in accumulation of endogenous L-3,4-dihydroxyphenylalanine (DOPA)- and dopamine (DA)-chromes derived from auto-oxidation of DOPA/DA-quinones, which mediates the toxic effect by covalently binding to the thiol group of proteins and consequently disintegrates cellular integrity and eventually causes cell death [18–20]. α-SN is a putative protein associated with membrane transport or signal transduction but of unknown function. α-SN gene mutations such as missense or multiplication cause familial autosomal dominant PD [21–27]. We found that forced expression of α-SN suppressed the loss of cell viability and accumulation of oxidative DOPA/DA metabolites caused by loss of parkin. Based on these findings, we propose that parkin and α-SN contribute to a common DA metabolic pathway; the impairment of which may lead to selective degeneration of dopaminergic neurons and consequently to PD.

Materials and methods

Adenoviruses. We used the adenoviral plasmid (pAdEasy-1) and the shuttle vector (p-shuttle-CMV) (Q.Bio gene). Various cDNAs used were inserted into the shuttle vector. The shuttle vector plasmid was linearized with *Pme*I. Electrocompetent *Escherichia coli* BJ5183 cells were added and electroporation was performed in 2-mm cuvettes in a Gene Pulser electroporator. Cells were inoculated onto 10-cm Petri dish containing LB-agar and 50 μg/ml kanamycin. Smaller colonies were picked and grown in 2 ml LB-broth (Sigma Chemical St. Louis, MO) containing 50 μg/ml kanamycin. Recombination was confirmed with *Pac*I. Approximately 5×10^6 cells were plated onto 10-cm culture dish. Ten micrograms of plasmid DNA linearized by *Pme*I, 12 μl FuGENE6 (Roche Molecular Systems, NJ), and 500 μl OptiMEM (Gibco-BRL) were mixed and transfected, according to the protocol provided by the manufacturer. After 7–10 days, the cells were collected by scraping off the 10-cm dish together with floating cells in the culture. The supernatant was removed after low-speed centrifugation. After sonicating the pellet, the cells were resuspended into 1 ml Dulbecco's modified Eagle's medium (DMEM) and frozen to −80 °C. In the next step, 500 μl of viral lysate was used to infect 7×10^7 cells in 15-cm dish. This process was repeated 1–3 times. Viruses were purified by CsCl banding; the final yield was 10^{10} plaque forming units.

Cells and cell culture. Human neuroblastoma cells (SH-SY5Y) and HeLa cells were obtained from American Type Culture Collection. The cells were maintained in growth medium (DMEM, Sigma, supplemented with 10% fetal bovine serum [Gibco-BRL, Gaithersburg, MD], 100 U/ml penicillin, and 100 μg/ml streptomycin) at 37 °C under 5% CO_2. SH-SY5Y cells were cultured with 100 μM of all *trans*-retinoic acid in dimethyl sulfoxide (DMSO) (Sigma R-2625) for 3 to 4 days for differentiation. The cells were infected with the antisense adenovirus at 150 moi; LacZ at 150 and 5 moi, wild and mutant α-SN adenovirus at 5 moi. Cells were collected 36 h after infection, centrifuged, and analyzed.

Western blotting. Infected or control cells were lysed in Laemmli SDS sample buffer. Proteins were separated by sodium dodecyl sulfate–polyacrylamide gel electrophoresis (SDS–PAGE) (NuPAGE, Invitrogen, San Diego, CA) and transferred onto polyvinylidene difluoride (PVDF) membrane. Western blotting was performed according to the ECL protocol provided by the supplier (Invitrogen, San Diego, CA) using specific antibodies of parkin and cleaved caspases (Cell Signaling Technology, Beverly, MA), α-SN (BD Transduction Laboratories, Lexington, KY), and β-Gal (Promega, Madison, WI).

Cell survival assay. Cells were infected with as-parkin or LacZ adenovirus and incubated for 48 h in 96-well plate. Cell viability was evaluated using the WST8, MTT reduction assay. Briefly, the solution of 0.1 mg/ml MTT in DMEM was added to each well and incubated for 2 h. The transmission was evaluated at 450 and 655 nm by 96-well microplate reader (Bio-Rad, Richmond, CA).

TUNEL assay. Terminal-deoxynucleotidyl transferase mediated d-UTP nick end labeling (TUNEL) assay was performed using formalin-fixed, ApopTag In Situ Apoptosis Detection Kits (Intergen, Purchase, NY). Fragmented DNA was labeled by fluorescein isothiocyanate (FITC) and observed under a fluorescence microscope.

Measurements of DOPA/DA-chromes. Thirty-six hours after infection, cells were solubilized in 500 μl of 1% Triton X-100 solution for 2 h and then centrifuged at 20,000*g* for 30 min at 4 °C. The supernatant was used as cell extract and was incubated for 3 min at room temperature. After 10% TCA protein precipitation, the generation of DOPA/DA-quinones was estimated by measuring the absorbance of the incubation supernatant at 475 nm based on the formation of DOPA/DA-chromes. The amount of DOPA/DA-chromes was calculated from a standard curve constructed using known amounts of DA and 0.01 mg/ml tyrosinase. The protein concentration in the cell extracts was determined by using the BCA Protein Assay Reagent Kit

(Pierce Chemical, Rockford, IL) with bovine serum albumin as a standard.

Statistical analysis. All data were expressed as means ± SEM. Differences between groups were examined for statistical significance using Dunnett's t test or Turkey's multiple t test. A P value less than 0.05 denoted the presence of a statistically significant difference.

Results and discussion

Antisense parkin causes loss of viability of SH-SY5Y cells

We first examined the effect of knockdown of parkin on the viability of human neuroblastoma cells (SH-SY5Y). These cells contain dopaminergic machinery and can differentiate into neuronal-like phenotypes when treated for 3–5 days with retinoic acid (RA), accompanied by arrest of cell proliferation and increased dopamine metabolism [28,29]. Infection of SH-SY5Y with full-length human as-parkin adenovirus caused deterioration of cell viability, as monitored by 3-(4,5-dimethylthiazol-2-yl)-2,5-diphenyltetrazolium bromide (MTT) reduction assay. The differential SH-SY5Y cell death effect was observed in the range between 50 and 250 moi titer of as-parkin adenovirus (data not shown) and thereafter we routinely used 150 moi titer (Fig. 1A, left panel). Control β-galactosidase (β-Gal) adenovirus had no effect on cell viability, although β-Gal was highly expressed in SH-SY5Y cells (Fig. 1A, right panel). Infection of cells with as-parkin caused a marked decrease of endogenous parkin protein level in differentiated SH-SY5Y cells, without altering actin level in the cells (Fig. 1A, right panel). The effect of as-parkin was abrogated, upon co-infection with sense-parkin (data not shown).

Effect of antisense parkin is cell-type specific

Intriguingly, we found that the effect of as-parkin on cell viability was much less in undifferentiated growing SH-SY5Y cells compared with differentiated cells (Fig. 1B, left panel). In addition, as-parkin did not influence cell viability of HeLa cells derived from human adenocarcinoma of the uterine cervix, which do not express parkin protein and lack the dopamine metabolic pathway (Fig. 1B, right panel). Thus, antisense knockdown of parkin exerts its effect based on the cell type, and the effects are observed in a dopaminergic neuron-specific manner, and depend on the differentiation state of dopaminergic neurons.

Antisense parkin induces apoptotic cell death

As shown in Fig. 1C, the cells appeared clear when their morphology was compared with uninfected (control) and β-Gal expressing cells. SH-SY5Y cells infected with as-parkin adenovirus showed morphological

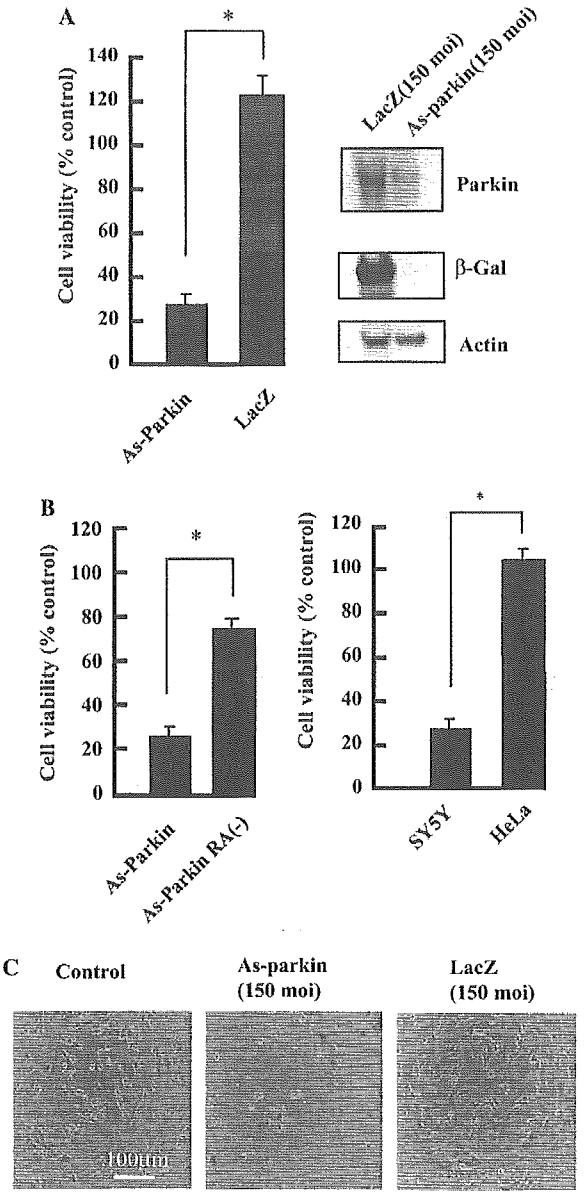

Fig. 1. Parkin knockdown is associated with loss of SH-SY5Y cell viability. (A) Effects of antisense parkin (as-parkin) and LacZ. Adenoviruses were infected for 48 h with 150 moi titers as indicated on the differentiated SH-SY5Y cells that had been pre-cultured with RA for 4 days. Cell viability was determined by the MTT assay (left panel). The results are expressed as percentage of MTT activity of uninfected cells (control). Data represent means ± SEM of 8 determinations. $*P < 0.01$ versus control group (Dunnett's t test). Cells that had been treated for 48 h with 150 moi titers of as-parkin and LacZ adenoviruses were lysed in Laemmli SDS sample buffer, and the proteins were separated by SDS–PAGE, followed by Western blotting with antibodies against parkin, β-galactosidase (β-Gal), and actin (right panel). (B) Undifferentiated SH-SY5Y cells without treatment with RA and HeLa cells were treated for 48 h with as-parkin adenovirus. The cell viability was measured and represented as indicated. (C) Morphological changes in differentiated SH-SY5Y cells upon knockdown of parkin. The cells were infected for 48 h with as-parkin and LacZ adenovirus vectors or left uninfected (control). Note the presence of apoptotic cells. Bar, 100 μm.

changes typical of apoptosis. To determine the nature of cell death induced by as-parkin, we performed TUNEL assay. As shown in Fig. 2A, as-parkin-treated SH-SY5Y cells showed nuclear condensation and fragmentation. In contrast, these changes were rarely observed in β-Gal-expressing SH-SY5Y cells. In support

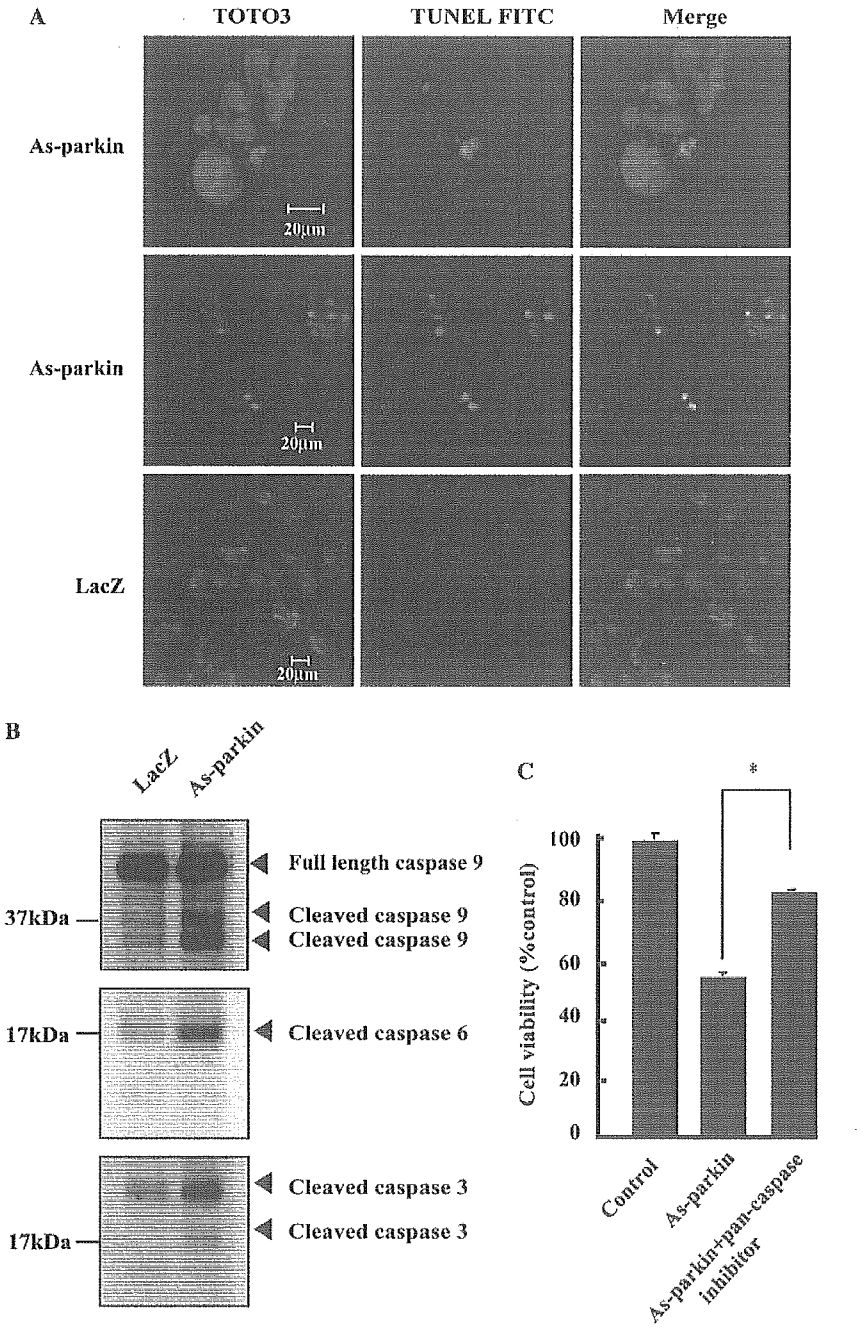

Fig. 2. Parkin knockdown induces apoptosis. (A) Detection of cells with nuclear DNA fragmentation due to parkin knockdown by TUNEL assay. Differentiated SH-SY5Y cells were treated for 48 h with as-parkin and LacZ adenoviruses (150 moi). TUNEL assay was performed to detect apoptotic cells. TUNEL-positive cells (green) were detected (TdT enzyme is labeled with FITC green fluorescence). Nuclei were counterstained with TOTO3 (red). Bar, 20 μm. (B) Activation of caspase-3, -6, and -9 by as-parkin. After infection with as-parkin and LacZ adenoviruses as for a, the cell extracts were used for Western blot analysis using antibodies against cleaved caspase-3, -6, and -9. Arrowheads on the right indicated corresponding caspases. Note that anti-cleaved caspase-3 and -6 antibodies did not react with their native forms. (C) Effects of a 'pan' caspase inhibitor on apoptosis induced by the loss of parkin. The inhibitor was added at 100 μM when cells were treated by as-parkin adenovirus as for (A). Note that the caspase inhibitor significantly blocked parkin knockdown-induced deterioration of cell viability. Data represent means ± SEM of 8 determinations. $^*P < 0.05$ versus control (uninfected) group (Dunnett's t test).

of the TUNEL findings, we also detected activation of caspase-3, -6, and -9 in SH-SY5Y cells under parkin knockdown (Fig. 2B). In addition, Western blot analysis showed cleaved poly(ADP)-ribose polymerase (PARP) in the course of as-parkin infection and a time-dependent increase of the 25-kDa cleaved fragment, confirming the activation of caspase(s) (data not shown). Further experiments showed that application of a pan-caspase inhibitor for 6 h before infection significantly prevented apoptotic cell death as determined by the MTT reduction assay (Fig. 2C). Taken together, these results suggest that as-parkin-induced SH-SY5Y cell death is likely to be mediated by activation of the caspase cascade.

Antisense parkin increases DOPA/DA metabolites

Next we examined the effect of α-SN on the viability and DOPA/DA-chrome level in differentiated SH-SY5Y cells with a reference to parkin loss. These experiments were based on previous studies describing abnormal DA metabolism in α-SN-deficient mice [30] and α-SN binding to DA-quinones [31]. For this purpose, we constructed adenovirus vectors expressing α-SN, and first tested its effect on the expression of parkin. α-SN and its PD-linked mutants (Ala30Pro and Ala53Thr) had no effect on the levels of parkin, irrespective of the treatment of as-parkin (Figs. 4A and B). It is of note that α-SN did not express at significant levels in SH-SY5Y cells under present conditions. Then, we investigated the effect of α-SN on the as-parkin-induced loss of cell viability. As shown in Fig. 4A, infection of SH-SY5Y cells by both adenovirus vectors expressing α-SN and as-parkin caused marked reduction of their cellular chrome levels and resulted in amelioration of as-parkin-induced deterioration of cell viability (Fig. 4B). Intriguingly, coinfection of cells with wild-type α-SN and as-parkin adenoviruses abrogated as-parkin-induced accumulation of DOPA/DA-chrome. However, α-SN mutants (Ala30Pro and Ala53Thr) and β-Gal expression did not reduce the generation of DOPA/DA-chrome by as-parkin. Thus, it seems that the α-SN-induced suppression of apoptosis was associated with a reduction in the DOPA/DA-chrome level in α-SN expressing SH-SY5Y cells. These results suggest that α-SN inhibits apoptosis induced by parkin knockdown by blocking the generation of DOPA/DA-chromes; i.e., DOPA/DA-quinones.

Antisense parkin-induced extensive apoptosis of differentiated dopaminergic SH-SY5Y cells but limited apoptosis of undifferentiated SH-SY5Y cells and no apoptosis of HeLa cells, indicating cell-type specificity. With regard to the cell-specific vulnerability, an important factor seems to be dopamine (DA) metabolism, which is a peculiar feature of dopaminergic neurons. Indeed, the differentiated SH-SY5Y cells retain a high DA metabolic pathway [28,29]. DA is a molecule prone to oxidation and it contributes to the generation of reactive oxygen species, which when in abundance can cause oxidative injury of various cellular components[18,20]. Indeed, abnormally high levels of these free radicals in dopaminergic neurons have been implicated as environmental factors causing not only sporadic PD but also AR-JP [32,33]. We tested the effects of as-parkin infection on the level of endogenous DOPA- and DA-chromes (DOPA/DA-chromes), which are derived from DOPA- and DA-quinones, respectively, whose metabolites could originate from cytosolic DOPA or DA oxidation [18,20]. Thus, the amounts of DOPA/DA-chromes reflect those of endogenous DOPA/DA-quinones. DOPA/DA-chrome levels were significantly high in parkin knockdown cells whereas there was no change in β-Gal expressing ones (Fig. 4A). These findings suggest that parkin knockdown-induced apoptosis is mediated by an increase in DOPA/DA-chromes.

Recently, four groups independently reported the generation of a mouse model that lacks the *parkin* gene, which display certain abnormalities of dopamine metabolism [34–37]. However, these parkin knockout mice had only subtle phenotypes exhibiting a largely normal gross brain morphology. Based on the pathologic findings, all the parkin null mice showed no neuronal loss in the SN. This is in marked contrast to our in vitro system described in this study, in which parkin knockdown induced activation of the caspase cascade and apoptosis of dopaminergic SH-SY5Y cells. Why do parkin knockout mice lack the abnormalities seen in AR-JP patients? One plausible explanation is the presence of a putative molecule(s) that suppresses the defect induced by loss-of-function of parkin, and the abundant presence of such molecule(s) in the brain should be linked to the pathogenesis of PD. Here, we propose that α-SN is the molecule that compensates for the loss of parkin, since α-SN prevented apoptotic cell death induced by as-parkin. In this regard, Western blot analysis showed that the dopaminergic SH-SY5Y cells did not express α-SN at significant levels (Fig. 3A, lanes 2 and 4), which is in marked contrast to the high abundance of dopaminergic neurons in vivo [38]. Regardless of the compensatory role of α-SN for the loss-of-function of parkin in the AR-JP, α-SN probably cannot cope with the accumulation of toxic molecules in the absence of parkin and thus apoptotic neuronal death perhaps occurs gradually, leading to degeneration of dopaminergic neurons and consequently the development of early-onset PD. We provide the first evidence for the anti-apoptotic role of α-SN and its involvement in the common pathway of parkin.

To date, several studies have demonstrated that α-SN exerts protective effects against various cellular stresses such as oxidative damage and related apoptosis of neurons [39,40]. Considering the reason why muta-

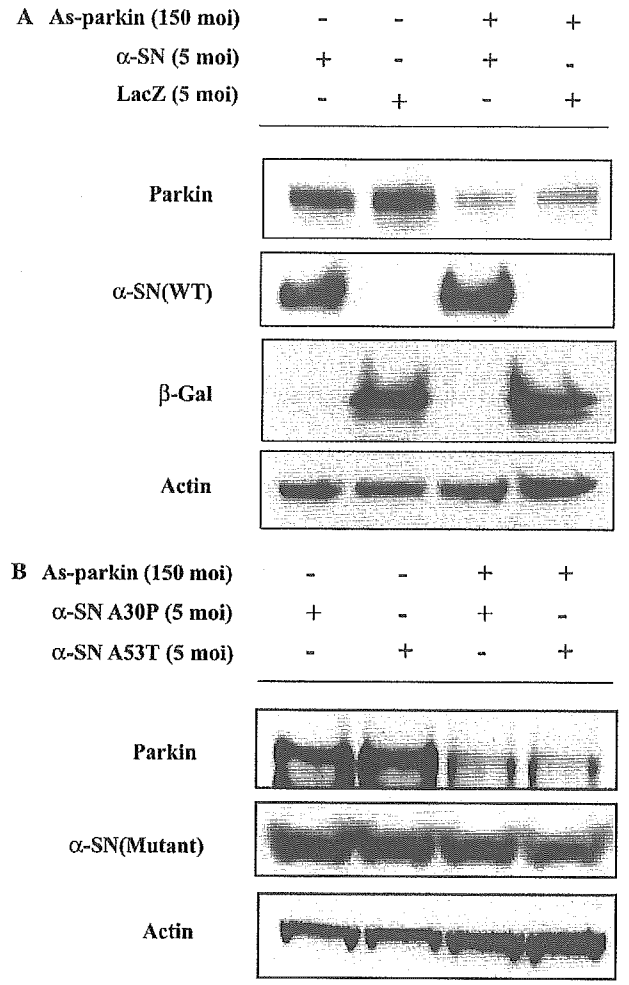

Fig. 3. Expression levels of parkin, α-SN, and LacZ. The expression levels of parkin, wild, and mutant α-SN, and LacZ in SH-SY5Y cells treated for 48 h with adenoviruses were monitored by Western blot analysis.

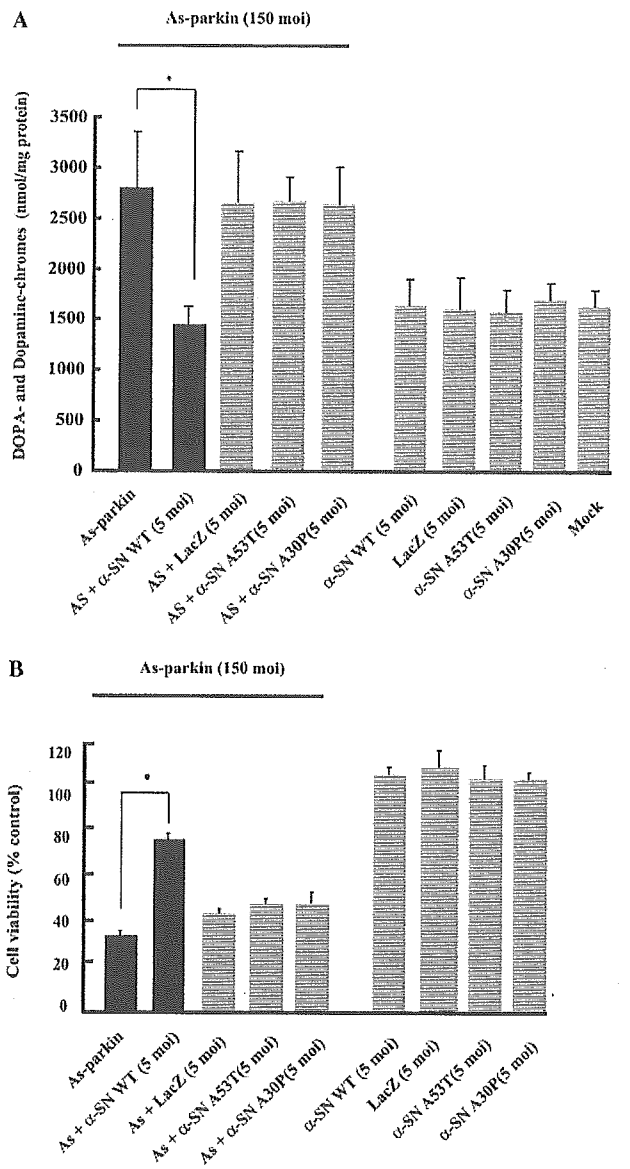

Fig. 4. α-Synuclein inhibits parkin knockdown-induced apoptosis and accumulation of DOPA- and DA-quinones. (A) Cellular level of DOPA/DA-chromes. After the differentiated SH-SY5Y cells were treated for 36 h with as-parkin, wild, and mutant α-SN, LacZ, and adenoviruses, cellular DOPA/DA-chromes were measured. Note the profound decrease of DOPA/DA-chromes in α-SN-expressing SH-SY5Y cells. Data are means ± SEM of 10 determinations. $^{*}P < 0.05$ versus control group (Turkey's multiple t test). (B) Effects of overexpression of wild and mutant α-SN on as-parkin-induced deterioration of cell viability. Differentiated SH-SY5Y cells were treated for 48 h with as-parkin adenovirus. Cells were coinfected with LacZ and α-SN adenovirus (5 moi) and at 150 moi titers of as-parkin adenovirus. The cell viability was measured and represented as in Fig. 1A (left panel).

tion of α-SN causes familial PD, it is clear that this type of disease is due to the gain-of-toxic function of the α-SN mutants with missense mutations, differing from the neuroprotective roles of the wild-type α-SN. In addition, α-SN proteins with disease-causing missense mutations tend to generate protofibrils [31,41], suggesting that protein misfolding including α-SN plays a key role in the pathogenesis of PD. In contrast, at high concentrations, it oligomerizes to β-pleated sheets known as protofibrils (i.e., fibrillar polymers with amyloid-like characteristics). Indeed, multiplication of α-SN has been reported in the autosomal dominant form of PD, indicating that overproduction of this protein affects the cellular damages. In this regard, there is a discrepancy between the protective role of α-SN in the present study and combination of PD and α-SN multiplication. This could be explained by appropriate physiological level of synuclein [40]. Thus, in patients with α-SN multiplication, the copy numbers of this gene may be related to the clinical severity of PD; patients with triplicate α-SN show dementia with Lewy bodies [24]; while those with duplicate levels do not show dementia [26,27].

It remains unclear why dopaminergic neurons of the substantia nigra are selectively vulnerable to the loss of parkin in AR-JP patients. In the present study, we provided a clue for this enigmatic puzzle. Considering the specificity of the lesions in PD, it is possible that the high oxidative state associated with DA metabolism may cause deterioration of dopaminergic neurons. The mechanism underlying increased oxidative stress may involve DA itself, because oxidation of cytosolic DOPA/DA may be deleterious to neurons. Indeed, DA causes apoptotic cell death as evident by morphological nuclear changes and DNA fragmentation [42–44]. In this regard, we showed here that as-parkin directed loss of parkin leads to abnormality of DOPA/DA metabolism, which resulted in the generation of DOPA/DA-quinones in SH-SY5Y cells. Thus, DA and its metabolites seem to exert cytotoxicity mainly by generating highly reactive quinones through auto-oxidation. On the other hand, the toxicity of DOPA and DA is due to the generation of reactive oxygen species that could disrupt cellular integrity, causing cell death. However, the reason for the production of oxidative DOPA/DA-metabolites following loss of parkin is not clear at present.

Our results showed for the first time that loss of parkin leads to death of differentiated dopaminergic cells in vitro. This cell-based experiment enhances our understanding of the pathophysiology of PD and could be potentially useful for drug screening. Our results also showed that α-SN and parkin are involved in DA metabolism and that aberrant regulation of DA is accompanied by accumulation of oxidative DOPA/DA metabolites.

Acknowledgments

This work was supported in part by Grants-in-Aid from the Ministry of Education, Culture, Sports, Science and Technology of Japan.

References

[1] T. Gasser, Genetics of Parkinson's disease, J. Neurol. 248 (2001) 833–840.
[2] T.M. Dawson, V.L. Dawson, Rare genetic mutations shed light on the pathogenesis of Parkinson disease, J. Clin. Invest. 111 (2003) 145–151.
[3] M.B. Feany, New genetic insights into Parkinson's disease, N. Engl. J. Med. 351 (2004) 1937–1940.
[4] T. Kitada, S. Asakawa, N. Hattori, H. Matsumine, Y. Yamamura, S. Minoshima, M. Yokochi, Y. Mizuno, N. Shimizu, Mutations in the parkin gene cause autosomal recessive juvenile parkinsonism, Nature 392 (1998) 605–608.
[5] H. Shimura, N. Hattori, S. Kubo, Y. Mizuno, S. Asakawa, S. Minoshima, N. Shimizu, K. Iwai, T. Chiba, K. Tanaka, T. Suzuki, Familial Parkinson disease gene product, parkin, is a ubiquitin–protein ligase, Nat. Genet. 25 (2000) 302–305.
[6] A. Hershko, A. Ciechanover, The ubiquitin system, Annu. Rev. Biochem. 67 (1998) 425–479.
[7] K. Tanaka, T. Suzuki, T. Chiba, The ligation systems for ubiquitin and ubiquitin-like proteins, Mol. Cells 8 (1998) 503–512.
[8] T.M. Dawson, V.L. Dawson, Molecular pathways of neurodegeneration in Parkinson's disease, Science 302 (2003) 819–822.
[9] Y. Zhang, J. Gao, K.K. Chung, H. Huang, V.L. Dawson, T.M. Dawson, Parkin functions as an E2-dependent ubiquitin–protein ligase and promotes the degradation of the synaptic vesicle-associated protein, CDCrel-1, Proc. Natl. Acad. Sci. USA 97 (2000) 13354–13359.
[10] A. Ciechanover, Linking ubiquitin, parkin and synphilin-1, Nat. Med. 7 (2001) 1108–1109.
[11] K.K. Chung, Y. Zhang, K.L. Lim, Y. Tanaka, H. Huang, J. Gao, C.A. Ross, V.L. Dawson, T.M. Dawson, Parkin ubiquitinates the alpha-synuclein-interacting protein, synphilin-1: implications for Lewy-body formation in Parkinson disease, Nat. Med. 7 (2001) 1144–1150.
[12] H. Shimura, M.G. Schlossmacher, N. Hattori, M.P. Frosch, A. Trockenbacher, R. Schneider, Y. Mizuno, K.S. Kosik, D.J. Selkoe, Ubiquitination of a new form of alpha-synuclein by parkin from human brain: implications for Parkinson's disease, Science 293 (2001) 263–269.
[13] Y. Imai, M. Soda, H. Inoue, N. Hattori, Y. Mizuno, R. Takahashi, An unfolded putative transmembrane polypeptide, which can lead to endoplasmic reticulum stress, is a substrate of Parkin, Cell 105 (2001) 891–902.
[14] J.F. Staropoli, C. McDermott, C. Martinat, B. Schulman, E. Demireva, A. Abeliovich, Parkin is a component of an SCF-like ubiquitin ligase complex and protects postmitotic neurons from kinate excitotoxicity, Neuron 37 (2003) 735–749.
[15] D. Yao, Z. Gu, T. Nakamura, Z.Q. Shi, Y. Ma, B. Gaston, L.A. Palmer, E.M. Rockenstein, Z. Zhang, E. Masliah, T. Uehara, S.A. Lipton, Nitrosative stress linked to sporadic Parkinson's disease: S-nitrosylation of parkin regulates its E3 ubiquitin ligase activity, Proc. Natl. Acad. Sci. USA 101 (2004) 10810–10814.
[16] K.K. Chung, B. Thomas, X. Li, O. Pletnikova, J.C. Troncoso, L. Marsh, V.L. Dawson, T.M. Dawson, S-nitrosylation of parkin regulates ubiquitination and compromises parkin's protective function, Science 304 (2004) 1328–1331.
[17] A. Yamamoto, A. Friedlein, Y. Imai, R. Takahashi, P.J. Kahle, C. Haass, Parkin phosphorylation and modulation of its E3 ubiquitin ligase activity, J. Biol. Chem. (2004).
[18] M. Asanuma, I. Miyazaki, N. Ogawa, Dopamine- or D-DOPA-induced neurotoxicity: the role of dopamine quinone formation and tyrosinase in a model of Parkinson's disease, Neurotox. Res. 5 (2003) 165–176.
[19] Y. Higashi, M. Asanuma, I. Miyazaki, N. Ogawa, Inhibition of tyrosinase reduces cell viability in catecholaminergic neuronal cells, J. Neurochem. 75 (2000) 1771–1774.
[20] D. Sulzer, L. Zecca, Intraneuronal dopamine-quinone synthesis: a review, Neurotox. Res. 1 (2000) 181–195.
[21] M.H. Polymeropoulos, C. Lavedan, E. Leroy, S.E. Ide, A. Dehejia, A. Dutra, B. Pike, H. Root, J. Rubenstein, R. Boyer, E.S. Stenroos, S. Chandrasekharappa, A. Athanassiadou, T. Papapetropoulos, W.G. Johnson, A.M. Lazzarini, R.C. Duvoisin, G. Di Iorio, L.I. Golbe, R.L. Nussbaum, Mutation in the alpha-synuclein gene identified in families with Parkinson's disease, Science 276 (1997) 2045–2047.
[22] M.C. Chartier-Harlin, J. Kachergus, C. Roumier, V. Mouroux, X. Douay, S. Lincoln, C. Levecque, L. Larvor, J. Andrieux, M. Hulihan, N. Waucquier, L. Defebvre, P. Amouyel, M. Farrer, A. Destee, Alpha-synuclein locus duplication as a cause of familial Parkinson's disease, Lancet 364 (2004) 1167–1169.
[23] A.D. Hope, R. Myhre, J. Kachergus, S. Lincoln, G. Bisceglio, M. Hulihan, M.J. Farrer, Alpha-synuclein missense and multipli-

cation mutations in autosomal dominant Parkinson's disease, Neurosci. Lett. 367 (2004) 97–100.
[24] A.B. Singleton, M. Farrer, J. Johnson, A. Singleton, S. Hague, J. Kachergus, M. Hulihan, T. Peuralinna, A. Dutra, R. Nussbaum, S. Lincoln, A. Crawley, M. Hanson, D. Maraganore, C. Adler, M.R. Cookson, M. Muenter, M. Baptista, D. Miller, J. Blancato, J. Hardy, K. Gwinn-Hardy, Alpha-synuclein locus triplication causes Parkinson's disease, Science 302 (2003) 841.
[25] D.W. Miller, S.M. Hague, J. Clarimon, M. Baptista, K. Gwinn-Hardy, M.R. Cookson, A.B. Singleton, Alpha-synuclein in blood and brain from familial Parkinson disease with SNCA locus triplication, Neurology 62 (2004) 1835–1838.
[26] P. Ibanez, A.M. Bonnet, B. Debarges, E. Lohmann, F. Tison, P. Pollak, Y. Agid, A. Durr, A. Brice, Causal relation between alpha-synuclein gene duplication and familial Parkinson's disease, Lancet 364 (2004) 1169–1171.
[27] J. Bradbury, Alpha-synuclein gene triplication discovered in Parkinson's disease, Lancet Neurol. 2 (2003) 715.
[28] H. Ikeda, A. Pastuszko, N. Ikegaki, R.H. Kennett, D.F. Wilson, 3,4-dihydroxyphenylalanine (dopa) metabolism and retinoic acid induced differentiation in human neuroblastoma, Neurochem. Res. 19 (1994) 1487–1494.
[29] M. Encinas, M. Iglesias, Y. Liu, H. Wang, A. Muhaisen, V. Cena, C. Gallego, J.X. Comella, Sequential treatment of SH-SY5Y cells with retinoic acid and brain-derived neurotrophic factor gives rise to fully differentiated, neurotrophic factor-dependent, human neuron-like cells, J. Neurochem. 75 (2000) 991–1003.
[30] A. Abeliovich, Y. Schmitz, I. Farinas, D. Choi-Lundberg, W.H. Ho, P.E. Castillo, N. Shinsky, J.M. Verdugo, M. Armanini, A. Ryan, M. Hynes, H. Phillips, D. Sulzer, A. Rosenthal, Mice lacking alpha-synuclein display functional deficits in the nigrostriatal dopamine system, Neuron 25 (2000) 239–252.
[31] K.A. Conway, J.C. Rochet, R.M. Bieganski, P.T. Lansbury Jr., Kinetic stabilization of the alpha-synuclein protofibril by a dopamine-alpha-synuclein adduct, Science 294 (2001) 1346–1349.
[32] P. Jenner, Oxidative stress in Parkinson's disease, Ann. Neurol. 53 (Suppl. 3) (2003) S26–S36, discussion S36–S28.
[33] Y. Zhang, V.L. Dawson, T.M. Dawson, Oxidative stress and genetics in the pathogenesis of Parkinson's disease, Neurobiol. Dis. 7 (2000) 240–250.
[34] J.M. Itier, P. Ibanez, M.A. Mena, N. Abbas, C. Cohen-Salmon, G.A. Bohme, M. Laville, J. Pratt, O. Corti, L. Pradier, G. Ret, C. Joubert, M. Periquet, F. Araujo, J. Negroni, M.J. Casarejos, S. Canals, R. Solano, A. Serrano, E. Gallego, M. Sanchez, P. Denefle, J. Benavides, G. Tremp, T.A. Rooney, A. Brice, J. Garcia de Yebenes, Parkin gene inactivation alters behaviour and dopamine neurotransmission in the mouse, Hum. Mol Genet. 12 (2003) 2277–2291.
[35] M.S. Goldberg, S.M. Fleming, J.J. Palacino, C. Cepeda, H.A. Lam, A. Bhatnagar, E.G. Meloni, N. Wu, L.C. Ackerson, G.J. Klapstein, M. Gajendiran, B.L. Roth, M.F. Chesselet, N.T. Maidment, M.S. Levine, J. Shen, Parkin-deficient mice exhibit nigrostriatal deficits but not loss of dopaminergic neurons, J. Biol. Chem. 278 (2003) 43628–43635.
[36] J.J. Palacino, D. Sagi, M.S. Goldberg, S. Krauss, C. Motz, M. Wacker, J. Klose, J. Shen, Mitochondrial dysfunction and oxidative damage in parkin-deficient mice, J. Biol. Chem. 279 (2004) 18614–18622.
[37] R. Von Coelln, B. Thomas, J.M. Savitt, K.L. Lim, M. Sasaki, E.J. Hess, V.L. Dawson, T.M. Dawson, Loss of locus coeruleus neurons and reduced startle in parkin null mice, Proc. Natl. Acad. Sci. USA 101 (2004) 10744–10749.
[38] R. Jakes, M.G. Spillantini, M. Goedert, Identification of two distinct synucleins from human brain, FEBS Lett. 345 (1994) 27–32.
[39] M. Hashimoto, L.J. Hsu, E. Rockenstein, T. Takenouchi, M. Mallory, E. Masliah, Alpha-synuclein protects against oxidative stress via inactivation of the c-Jun N-terminal kinase stress-signaling pathway in neuronal cells, J. Biol. Chem. 277 (2002) 11465–11472.
[40] J.H. Seo, J.C. Rah, S.H. Choi, J.K. Shin, K. Min, H.S. Kim, C.H. Park, S. Kim, E.M. Kim, S.H. Lee, S. Lee, S.W. Suh, Y.H. Suh, Alpha-synuclein regulates neuronal survival via Bcl-2 family expression and PI3/Akt kinase pathway, FASEB J. 16 (2002) 1826–1828.
[41] K.A. Conway, S.J. Lee, J.C. Rochet, T.T. Ding, R.E. Williamson, P.T. Lansbury Jr., Acceleration of oligomerization, not fibrillization, is a shared property of both alpha-synuclein mutations linked to early-onset Parkinson's disease: implications for pathogenesis and therapy, Proc. Natl. Acad. Sci. USA 97 (2000) 571–576.
[42] M. Emdadul Haque, M. Asanuma, Y. Higashi, I. Miyazaki, K. Tanaka, N. Ogawa, Apoptosis-inducing neurotoxicity of dopamine and its metabolites via reactive quinone generation in neuroblastoma cells, Biochim. Biophys. Acta 1619 (2003) 39–52.
[43] T.G. Hastings, D.A. Lewis, M.J. Zigmond, Role of oxidation in the neurotoxic effects of intrastriatal dopamine injections, Proc. Natl. Acad. Sci. USA 93 (1996) 1956–1961.
[44] D.C. Jones, P.G. Gunasekar, J.L. Borowitz, G.E. Isom, Dopamine-induced apoptosis is mediated by oxidative stress and Is enhanced by cyanide in differentiated PC12 cells, J. Neurochem. 74 (2000) 2296–2304.

Journal of Neurochemistry, 2005, **94**, 1254–1263 doi:10.1111/j.1471-4159.2005.03272.x

In vivo evidence of CHIP up-regulation attenuating tau aggregation

Naruhiko Sahara,* Miyuki Murayama,* Tatsuya Mizoroki,* Makoto Urushitani,† Yuzuru Imai,† Ryosuke Takahashi,†,[1] Shigeo Murata,‡ Keiji Tanaka‡ and Akihiko Takashima*

**Laboratory for Alzheimer's Disease and †Laboratory for Motor System Neurodegeneration. RIKEN Brain Science Institute, Saitama, Japan*

‡Department of Molecular Oncology, Tokyo Metropolitan Institute of Medical Science, Tokyo, Japan

Abstract

The carboxyl terminus of heat-shock cognate (Hsc)70-interacting protein (CHIP) is a ubiquitin E3 ligase that can collaborate with molecular chaperones to facilitate protein folding and prevent protein aggregation. Previous studies showed that, together with heat-shock protein (Hsp)70, CHIP can regulate tau ubiquitination and degradation in a cell culture system. Ubiquitinated tau is one component in neurofibrillary tangles (NFTs), which are a major histopathological feature of Alzheimer's disease (AD). However, the precise sequence of events leading to NFT formation and the mechanisms involved remain unclear. To confirm CHIP's role in suppressing NFT formation *in vivo*, we performed a quantitative analysis of CHIP in human and mouse brains. We found increased levels of CHIP and Hsp70 in AD compared with normal controls. CHIP levels in both AD and controls corresponded directly to Hsp90 levels, but not to Hsp70 or Hsc70 levels. In AD samples, CHIP was inversely proportional to sarkosyl-insoluble tau accumulation. In a JNPL3 mouse brain tauopathy model, CHIP was widely distributed but weakly expressed in spinal cord, which was the most prominent region for tau inclusions and neuronal loss. Protein levels of CHIP in cerebellar regions of JNPL3 mice were significantly higher than in non-transgenic littermates. Human tau was more highly expressed in this region of mouse brains, but only moderate levels of sarkosyl-insoluble tau were detected. This was confirmed when increased insoluble tau accumulation was found in mice lacking CHIP. These findings suggest that increases in CHIP may protect against NFT formation in the early stages of AD. If confirmed, this would indicate that the quality-control machinery in a neuron might play an important role in retarding the pathogenesis of tauopathies.

Keywords: Alzheimer's disease, carboxyl terminus of heat-shock cognate 70-interacting protein, heat-shock protein, molecular chaperone, neurofibrillary tangle, tau.

J. Neurochem. (2005) **94**, 1254–1263.

The carboxyl terminus of heat-shock cognate (Hsc)70-interacting protein (CHIP) is a key molecule in protein quality-control processes that links the ubiquitin–proteasome and chaperone systems (Murata *et al.* 2001). CHIP has the U-box domain that facilitates ubiquitin-conjugating enzyme (E2)-dependent ubiquitination (Hatakeyama *et al.* 2001). CHIP was originally discovered as a co-chaperone with a tetratricopeptide repeat-containing protein that negatively regulates the ATPase and chaperone activities of Hsc70 (Ballinger *et al.* 1999). The biochemical effects of CHIP have been well characterized using cell culture systems. Various molecules have been identified as CHIP substrates, including the glucocorticoid receptor (Connell *et al.* 2001), the misfolded cystic fibrosis transmembrane-conductance regulator (CFTR) (Meacham *et al.* 2001), heat-denatured luciferase (Murata *et al.* 2001), the transmembrane receptor tyrosine kinase ErbB2 (Xu *et al.* 2002)

Received February 16, 2005; revised manuscript received April 10, 2005; accepted April 26, 2005.

Address correspondence and reprint requests to Akihiko Takashima, Laboratory for Alzheimer's Disease, RIKEN Brain Science Institute, Wako-shi, Saitama 351–0198, Japan. E-mail: kenneth@brain.riken.jp

[1]The present address of Ryosuke Takahashi is the Department of Neurology, Graduate School of Medicine, Kyoto University, 54 Kawahara-cho, Shogoin, Sakyo-ku, Kyoto 606-8507, Japan.

Abbreviations used: AD, Alzheimer's disease; CFTR, cystic fibrosis transmembrane-conductance regulator; CHIP, carboxyl terminus of heat-shock cognate 70-interacting protein; Hsc, heat-shock cognate; HSF1, heat shock factor 1; Hsp, heat-shock protein; MES, 2-(N-Morpholino) ethanesulfonic Acid; NFT, neurofibrillary tangle; NSE, neuron-specific enolase; PAGE, polyacrylamide gel electrophoresis; PBS, phosphate-buffered saline; PHF, paired helical filaments; PHF-tau, PHF-1 antibody-immunoreactive tau; PMSF, phenylmethylsulfonyl fluoride; SDS, sodium dodecyl sulfate; TBS, Tris-buffered saline; Tg, transgenic.

and microtubule-associated protein tau (Petrucelli *et al.* 2004; Shimura *et al.* 2004). We found that CHIP directly mediates tau ubiquitination without heat-shock proteins (Hsps) *in vitro*, preferentially interacts with four-repeat tau, and protects against vulnerability of P301L mutated tau expressing cells (Hatakeyama *et al.* 2004). However, little is known about the biochemical features of CHIP in the brain. Only immunohistochemical analyses have been reported, including those that show anti-CHIP antibody-positive tau inclusions in several tauopathies including Alzheimer's disease (AD), progressive supranuclear palsy, corticobasal degeneration and Pick's disease (Hatakeyama *et al.* 2004; Petrucelli *et al.* 2004), and anti-CHIP antibody-positive Lewy body-like hyaline inclusions in a familial amyotrophic lateral sclerosis mouse model (Urushitani *et al.* 2004).

Tau is a neuronal microtubule-binding protein that normally enhances microtubule stability. However, it can be hyperphosphorylated in pathogenic conditions, and detach from microtubules and accumulate in the neurofibrillary tangles (NFTs) that are one of neuropathological hallmarks of AD (Grundke-Iqbal *et al.* 1986). Despite the suspected role of tau phosphorylation in NFT formation, the precise sequence of events leading to NFT formation and the mechanisms involved remain poorly understood. In addition to tau phosphorylation, other abnormal post-translational modifications have been observed including ubiquitination, glycosylation, glycation, polyamination, nitration and proteolysis (for review, see Gong *et al.* 2005). In most neurodegenerative diseases, anti-ubiquitin antibody- and anti-proteasome antibody-positive inclusions were detected in affected neurons (for review, see Sherman and Goldberg 2001), so the ubiquitin–proteasome may be one mechanism responsible for tau degradation in tauopathies. Various molecular chaperones were also colocalized in protein aggregates that are characteristic of neurodegenerative diseases (for review, see Muchowski and Wacker 2005). CHIP may attenuate NFT formation as a bridging mechanism between molecular chaperones and the ubiquitin–proteasome system.

In the present study, human AD brain, JNPL3 mice (Lewis *et al.* 2000) expressing human P301L mutant tau that is associated with frontotemporal dementia and parkinsonism linked to chromosome 17, and a novel *CHIP* knockout mouse were used to investigate the *in vivo* roles of CHIP in regulating tau ubiquitination, degradation and aggregation. We found increased levels of CHIP in AD brains that were inversely proportional to the amount of accumulated tau. The level of CHIP corresponded with the level of Hsp90 but not with that of Hsp70 or Hsc70. These *in vivo* studies of CHIP biochemistry suggest the existence of a Hsp90–CHIP chaperone system, which plays an ameliorating role in the early stages of tauopathies.

Materials and methods

Antibodies

Polyclonal CHIP antibodies (R1) were prepared in rabbits (Imai *et al.* 2002). Antiserum specific for recombinant CHIP with a His-Tag sequence was purchased from Calbiochem (La Jolla, CA, USA). E1 (Kenessey *et al.* 1997), a polyclonal antibody specific to human tau (amino acids 19–33, according to the numbering of a longest isoform of human tau unphosphorylated), was prepared in our laboratory. Polyclonal tau antibody tauC was raised against tau polypeptide corresponding to amino acid residues 422–438. Anti-Tau5 and pS199 (phosphorylation site at Ser199) were purchased from Biosource International (Camarillo, CA, USA). Anti-Tau1 was from Chemicon (Temecula, CA, USA). Monoclonal antibody to tau phosphorylated at ser396/Ser404 (PHF-1) was provided by Dr Peter Davies (Jicha *et al.* 1999). Monoclonal antibodies to Hsp90, Hsp70, β-actin, neuron-specific enolase (NSE) and ubiquitin were purchased from Santa Cruz Biotechnology (Santa Cruz, CA, USA), Chemicon, Sigma (St Louis, MO, USA) Upstate (Charlottesville, VA, USA) and MBL (Nagoya, Japan) respectively. Polyclonal antibody to Hsc70 was purchased from MBL. For western blotting, antibodies were used at the following dilutions in blocking solution: CHIP, 1 : 5000; E1, 1 : 5000; tauC, 1 : 5000; tau1, 1 : 2000; tau5, 1 : 2000; pS199, 1 : 5000; PHF-1, 1 : 2000; Hsp90, 1 : 2000; Hsp70, 1 : 1000; β-actin, 1 : 10 000; NSE, 1 : 1000; ubiquitin, 1 : 500; Hsc70, 1 : 1000.

Human brain

Temporal cortices from nine AD (AD1 to AD9) and six non-AD controls (C1 to C6) were obtained. They were processed for western blotting as described below. The age, sex and post-mortem intervals of each subject were: AD2, 85 years, male, 10 h; AD3, 77 years, female, 2.5 h; AD4, 66 years, female, 2.5 h; AD5, 79 years, male, 1.5 h; AD7, 66 years, male, 2.5 h; AD8, 60 years, female, 3 h; C1, 57 years, female, 8 h; C2, 69 years, male; C3, 69 years, male; C4, 68 years, male, 6 h; C6, 65 years, female. Information about remaining samples was not available (described in Yan *et al.* 1994).

JNPL3 mice and littermates

Female hemizygous JNPL3 mice (Tau MI with B6D2F1 background; Taconic Laboratories Germantown, NY, USA) were obtained at 8 weeks of age. JNPL3 mice express the 4R0N isoform of human P301L mutant tau and are characterized as developing NFTs, as well as sarkosyl-insoluble tau in an age-dependent manner (Lewis *et al.* 2001; Sahara *et al.* 2002). Transgenic (Tg) mice and non-Tg littermates were bred by mating hemizygous JNPL3 mice with C57BL/6J Jcl (Clea, Tokyo, Japan). Mice were genotyped for the *tau* transgene by PCR between exons 9 and 13 of human tau cDNA. Animals were housed under controlled conditions with a 12-h day–night cycle. They were killed between 1.5 and 11.6 months after birth. The age ranges of the JNPL3 mice were 1.5 months ($n = 2$), 4–5 months ($n = 2$), 6–7 months ($n = 3$), 8–9 months ($n = 3$) and 10–11 months ($n = 2$). The age ranges of non-Tg mice were 1.5 months ($n = 1$), 4–5 months ($n = 3$), 6–7 months ($n = 2$) and 8–9 months ($n = 3$). Procedures involving animals and their care were approved by the Animal Care and Use Committee of RIKEN.

Tissue extraction

Mouse brains were separated into eight regions: olfactory bulb, cerebral cortex, hippocampus, diencephalons, midbrain, pons and medulla oblongata, cerebellum and spinal cord. These regions were quickly frozen on dry ice and stored at −80°C. Each sample was homogenized subsequently in five volumes of Tris-buffered saline (TBS) containing protease and phosphatase inhibitors [25 mM Tris/HCl, pH 7.4, 150 mM NaCl, 1 mM EDTA, 1 mM EGTA, 5 mM sodium pyrophosphate, 30 mM β-glycerophosphate, 30 mM sodium fluoride and 1 mM phenylmethylsulfonyl fluoride (PMSF)]. The homogenates were centrifuged at 27 000 *g* for 15 min at 4°C to obtain a supernatant (TBS sup) and pellet fractions. Pellets were re-homogenized in five volumes of high-salt/sucrose buffer (0.8 M NaCl, 10% sucrose, 10 mM Tris/HCl, pH 7.4, 1 mM EGTA, 1 mM PMSF) and centrifuged as above. The supernatants were collected and incubated with sarkosyl (Sigma; 1% final concentration) for 1 h at 37°C, followed by centrifugation at 150 000 *g* for 1 h at 4°C to obtain salt and sarkosyl-soluble and sarkosyl-insoluble pellets (srk-ppt fractions). To determine the extent of post-mortem protein degradation, hemibrains were kept at room temperature (25°C) for various time intervals (1, 2, 4, 8, 24 and 70 h) after the death of 7-month-old female C57BL/6J mice. As a control, the other hemibrains were quickly frozen in dry ice and stored at −80°C. Each sample was homogenized in TBS buffer containing protease and phosphatase inhibitors, and was centrifuged at 27 000 *g* for 15 min at 4°C. The supernatants were used for western blot analysis.

CHIP knockout mice

The first six exons of the *CHIP* gene were replaced with a PGK-neo selection cassette by homologous recombination. Germline transfer of the targeted allele was successful. Mice heterozygous at the *CHIP* locus were maintained on a C57BL/6 background. Mice aged 2.5 months (wild type $n = 1$, heterozygous $n = 1$, homozygous $n = 1$) and 18 months (wild type $n = 4$, heterozygous $n = 4$, homozygous $n = 4$) were killed, and hemibrains were quickly frozen on dry ice and stored at −80°C. As described previously (Ishihara *et al.* 1999; Tanemura *et al.* 2002), tissue extracts were sequentially fractionated with the following buffers: reassembly buffer (RAB; 0.1 M 2-(N-Morpholino)ethanesulfonic Acid (MES), 1 mM EGTA, 0.5 mM $MgSO_4$, 0.75 M NaCl, 0.02 M NaF, 1 mM PMSF and protease inhibitor cocktail, pH 7.0), RAB containing 1 M sucrose, RIPA buffer [50 mM Tris, 150 mM NaCl, 1% NP-40, 5 mM EDTA, 0.5% sodium deoxycholate and 0.1% sodium dodecyl sulfate (SDS), pH 8.0], RIPA buffer containing 1% SDS, and TBS containing 1% SDS. The final pellet was solubilized in 70% formic acid and reconstituted in Laemmli SDS–polyacrylamide gel electrophoresis (PAGE) sample buffer after lyophilization.

Western blotting

Fractionated tissue extracts were dissolved in sample buffer containing β-mercaptoethanol (0.01%). The boiled extracts were separated by gel electrophoresis on 10% or 4–20% gradient SDS–PAGE gels, and transferred to nitrocellulose membranes (Schleicher & Schuell BioScience, Dassel, Germany). After blocking with a blocking solution containing 5% non-fat milk, 0.1% goat serum and 0.1% Tween-20 in phosphate-buffered saline (PBS), the membranes were incubated with various antibodies, washed to remove excess antibodies, and then incubated with peroxidase-conjugated goat anti-rabbit antibodies (1 : 5000; Jackson ImmunoResearch, West Grove, PA, USA) or anti-mouse IgG (1 : 5000; Jackson ImmunoResearch). Bound antibodies were detected using an enhanced chemiluminescence system, SuperSignal West Pico (Pierce Biotechnology, Rockford, IL, USA). For specificity testing of anti-CHIP antibody, pre-absorption was performed. Recombinant His-tagged CHIP was resuspended in 1% bovine serum albumin, 0.1% goat serum and 0.1% Tween-20 in PBS to a concentration of 40 μg/mL. The solution was added to dilute CHIP antibody to a final dilution of 1 : 5000. The mixture was rotated for 2 h at room temperature, then centrifuged at 12 000 *g* for 5 min. The supernatant was separated from the pellet and used for western blotting. Quantitation and visual analysis of immunoreactivity were performed with a computer-linked LAS-1000 Bio-Imaging Analyzer System (Fujifilm, Tokyo, Japan) using the software program Image Gauge 3.0 (Fujifilm).

Statistical analysis

The correlation between the levels of CHIP in AD brain and control brain, and between CHIP and Hsp levels, was tested by unpaired *t*-test with Welch correction. The correlation between the level of CHIP and PHF-tau was tested using Pearson correlation. Data were analyzed with InStat for Macintosh, version 3.0a (Graphpad, San Diego, CA, USA). The level of significance was set at $p < 0.05$.

Results

Identification of CHIP in brain extracts

CHIP, a 35-kDa cytoplasmic protein, is highly expressed in adult striated muscle with less expression in the pancreas and brain. It is also expressed broadly in tissue culture (Ballinger *et al.* 1999). Polyclonal CHIP antibodies from both laboratory and commercial sources were used for western blotting. Both were raised from full-length CHIP recombinant protein. Samples from human embryonic kidney (HEK)293 cells showed the strongest immunoreactive band with a mobility size of 35 kDa (Fig. 1a). Both mouse and human brain extracts showed a single 35-kDa band in the blot with R1 antibody. This band was absorbed by preincubation of primary antibody with recombinant protein. The blot with the Calbiochem antibody showed a 35-kDa band of the same intensity in each sample, but additional bands were detected. These data suggest that the 35-kDa band was the protein product of *CHIP* and that the R1 antibody is more specific to CHIP than the antibody from Calbiochem. We also detected doublet bands in human materials using the enlarged electrophoretic condition (Fig. 1b). For quantitative analysis, we excluded the upper band in human materials because the mobility of the lower band was same as the 35-kDa band in mouse brain (Fig. 1b) and all the human brain samples showed similar extensions of the upper band (Fig. 2a).

Levels of CHIP in AD brain were higher than levels in non-AD controls

Quantitative western blotting analyses revealed variable levels of the 35-kDa band in human brain extracts (Fig. 2a).

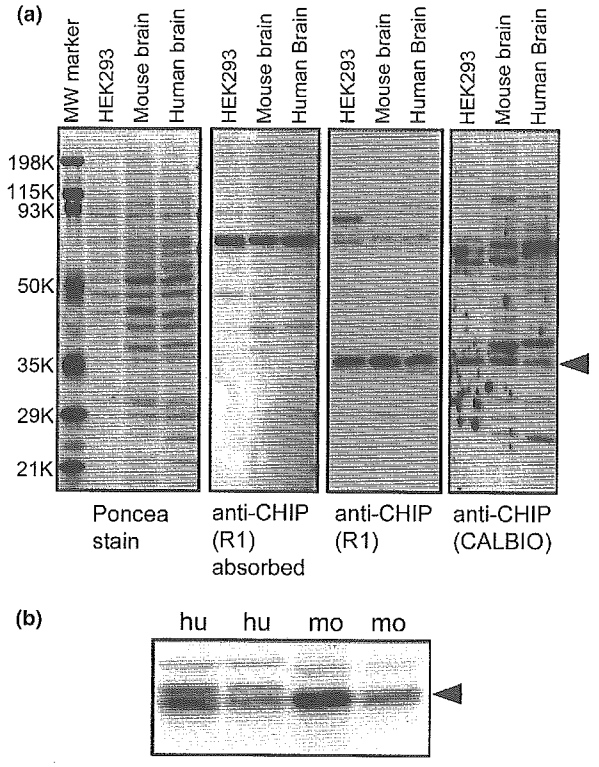

Fig. 1 Identification of CHIP using specific antibodies. (a) Replicated membranes containing human embryonic kidney (HEK)293 cells, mouse brain and human brain extracts were immunoblotted with anti-CHIP antibodies [preabsorbed R1, R1 and Calbiochem (CALBIO)]. One set of membranes was stained with poncea. A 35-kDa band (arrowhead) was detected with both R1 and Calbiochem antibodies but completely absorbed by recombinant CHIP. (b) Human brain extracts contained doublet bands. The lower band in human brain indicated by arrowhead was identical to the band in mouse brain.

Before making comparisons between AD and non-AD controls, both sarkosyl-insoluble tau and SDS-insoluble β-amyloid were analyzed by western blotting to confirm diagnostic information. PHF-1-positive triplet bands were detected in all nine AD cases but not in the non-AD controls when sarkosyl-insoluble fractions derived from over 40 mg wet-weight of brain tissue were loaded (data not shown). SDS-insoluble β-amyloid was detected in all AD cases and some non-AD controls (data not shown). To compare protein levels of CHIP and Hsp between AD and non-AD controls, the amount of β-actin was used for normalization of protein levels. Levels of CHIP were significantly higher in AD brain compared with non-AD controls ($p = 0.040$; unpaired t-test with Welch correction) (Fig. 2b). A significant increase in Hsp70 levels in AD compared with control brains was observed ($p = 0.0032$) (Fig. 2d), but no significant difference in either Hsp90 or Hsc70 ($p = 0.84$ and $p = 0.57$ respectively) (Fig. 2c). Comparing individual samples, CHIP and Hsp90 levels were directly related, but CHP levels were not related to those of either Hsp70 or Hsc70 (Figs 2a and e). The correlation between the levels of CHIP and Hsp90 was highly significant ($r = 0.71$, $p = 0.0029$, $n = 15$; Pearson correlation). When the amount of NSE was used for normalization, the same statistical results were obtained (data not shown).

Inverse relationship between CHIP and PHF-1 antibody-immunoreactive tau (PHF-tau) in AD brain

To determine whether NFT formation in AD brain is influenced by the protein level of CHIP, the amount of CHIP, normalized with respect to β-actin in the TBS-soluble fraction, was plotted against PHF-tau in the sarkosyl-insoluble fraction. These were samples that tested positive for highly phosphorylated tau. Although detailed information on the pathological course for each AD case was not available, the relative amount of PHF-tau revealed through biochemical studies provided detailed information about the NFT pathogenesis in each. This information correlated with the severity of disease (Dickson *et al.* 2000; Johnson and Bailey 2002). As shown in Fig. 2(a), the intensity of PHF-tau staining varied among the AD cases as did that of both CHIP and Hsp90. Interestingly, the amount of PHF-tau was inversely proportional to amount of CHIP ($r = -0.83$, $p = 0.0051$, $n = 9$; Pearson correlation) (Fig. 2f). As described previously, levels of Hsp90 in AD cases with mature PHF-tau accumulation were lower than those in immature or non-AD cases (Dou *et al.* 2003). Conversely, soluble tau levels were not influenced by either CHIP or Hsp90 levels. To determine whether the sequestration of CHIP with NFTs occurred during pathogenesis, we analyzed CHIP levels in the sarkosyl-insoluble fraction (Fig. 2a). Consistent with the results of the anti-CHIP blot of the TBS sup fraction, the level of sarkosyl-insoluble CHIP was inversely related to the PHF-tau level. Sarkosyl-insoluble CHIP in controls was also detected with similar intensity to that in AD cases. These data suggest that CHIP precipitated in this fraction in a PHF-tau-independent manner.

Effect of post-mortem interval on protein levels of CHIP

Large variations in CHIP and Hsp90 protein levels were found among control and AD brains (Fig. 2a). To exclude the possibility of post-mortem protein degradation, we attempted the comparative protein quantification of mouse brains with several post-mortem intervals. Coomassie Brilliant Blue staining of polyacrylamide gels showed visible protein degradation after a post-mortem interval of 24 h (Fig. 3). However, western blots for CHIP, Hsp90, Hsp70 and β-actin showed constant protein levels. Only tau protein levels were affected by the post-mortem interval. The observed mobility shift may correspond to dephosphorylation. These data strongly suggest that protein levels of CHIP and Hsps extracted from both human and mouse brains were not affected by the post-mortem interval.

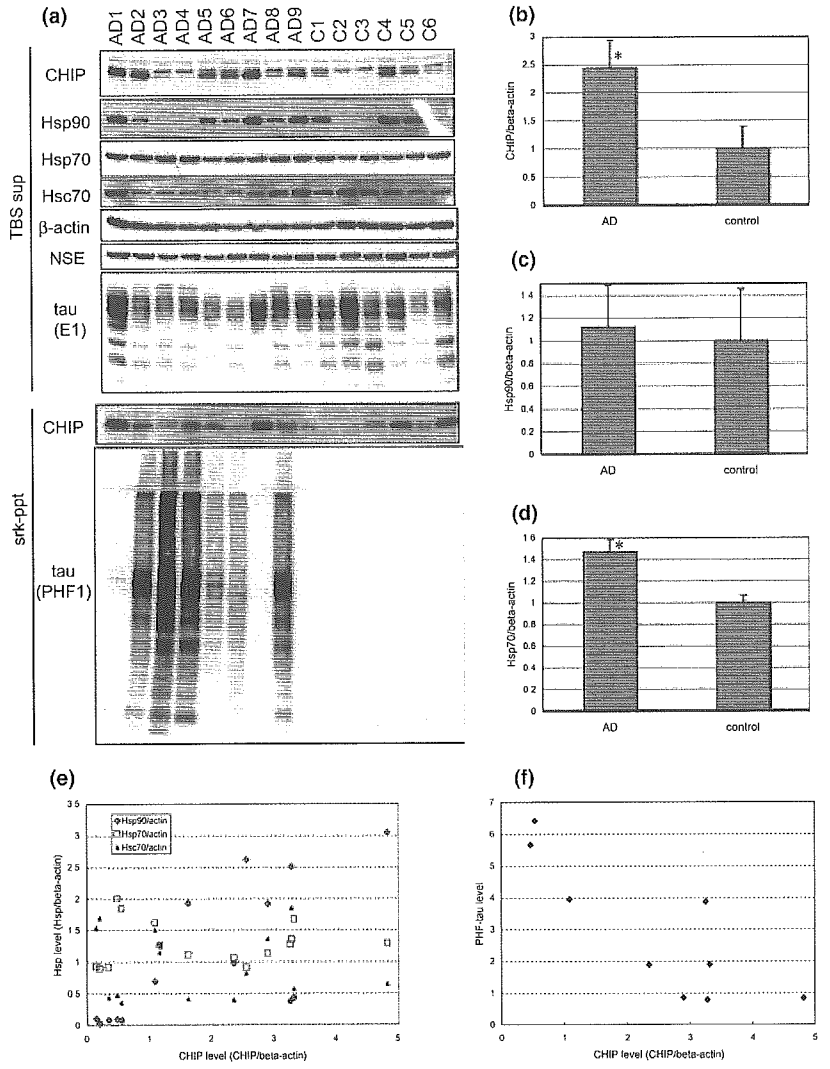

Fig. 2 Quantitative analysis of CHIP in human brains. (a) TBS-soluble fractions (TBS sup) from human temporal cortex from nine AD and six non-AD control cases were blotted using CHIP (R1), Hsp90, Hsp70, Hsc70, β-actin, NSE and E1 antibodies. Sarkosyl-insoluble fractions (srk-ppt) derived from 40 mg wet-weight of brain were blotted using CHIP (R1) antibodies and those derived from 4 mg wet-weight of brain were blotted using PHF-1 antibody. Amounts of CHIP (b), Hsp90 (c) and Hsp70 (d) normalized with respect to β-actin were analyzed. Values are mean ± SEM. $^*p < 0.05$ versus control (unpaired *t*-test with Welch correction). (e) Correlations between CHIP and Hsp90, Hsp70 or Hsc70 levels. (f) Amount of CHIP normalized with respect to β-actin in TBS-soluble fraction plotted against sarkosyl-insoluble PHF-tau level. $p < 0.01$ ($n = 9$; Pearson correlation).

Distribution of CHIP in mouse brain

Since the discovery of CHIP (Ballinger *et al.* 1999) and its role as E3 ligase (Hatakeyama *et al.* 2001; Jiang *et al.* 2001; Murata *et al.* 2001), little research has been conducted to determine its *in vivo* protein properties. In the present study the distribution of CHIP in mouse brain was investigated using biochemical strategies. CHIP was found to be highly expressed in the olfactory bulb, cerebral cortex, hippocampus and cerebellum, moderately expressed in the diencephalons, midbrain and pons/medulla oblongata, but weakly expressed in the spinal cord (Fig. 4a). Hsp90 was broadly expressed throughout the mouse brain, whereas Hsp70 was highly expressed in cerebral cortex and hippocampus with only moderate expression in other brain regions (Fig. 4a). The distribution patterns of the three chaperone-related proteins in mouse samples were not identical. CHIP distribution in mouse brain corresponded with tau distribution except in the olfactory bulb. The distribution patterns of CHIP, Hsp90 and Hsp70 did not vary with age or sex (data not shown).

Increased level of CHIP in JNPL3 mouse brain

To search for linkages between abnormal tau accumulation and CHIP expression, JNPL3 mouse brains were analyzed; 64-kDa tau was observed in the sarkosyl-insoluble fraction from the midbrain, pons/medulla oblongata and spinal cord regions of 9.5-month-old female JNPL3 mouse (Fig. 4b, middle panel). As described previously (Sahara *et al.* 2002), human P301L tau protein expression was higher in the hindbrain regions, including midbrain, pons/medulla oblongata, cerebellum and spinal cord, than in the forebrain regions, including cerebral cortex, hippocampus and diencephalons (Fig. 4b, upper panel). Interestingly, the cerebellum had the highest levels of exogenous tau protein but only moderate levels of sarkosyl-insoluble tau. The distribution pattern of